Prenatal programming by testosterone of follicular theca cell functions in ovary

Danielle Monniaux, Carine Genet, Virginie Maillard, Peggy Jarrier, Hans Adriaensen, Christelle Hennequet-Antier, Anne-Lyse Lainé, Corinne Laclie, Pascal Papillier, Florence Plisson-Petit, et al.

Prenatal programming by testosterone of follicular theca cell functions in ovary

Danielle Monniaux[1$], Carine Genêt[2], Virginie Maillard[1], Peggy Jarrier[1], Hans Adriaensen[1], Christelle Hennequet-Antier[3], Anne-Lyse Lainé[1], Corinne Laclie[1], Pascal Papillier[1], Florence Plisson-Petit[2], Anthony Estienne[1], Juliette Cognié[1], Nathalie di Clemente[4], Rozenn Dalbies-Tran[1$], Stéphane Fabre[2]

[1]UMR Physiologie de la Reproduction et des Comportements, INRA, CNRS, IFCE, Université de Tours, 37380 Nouzilly, France

[2]GenPhySE, Université de Toulouse, INRA, INPT, ENVT, 31320 Castanet Tolosan, France

[3]BOA, INRA, Université de Tours, 37380 Nouzilly, France

[4]Sorbonne Université, INSERM, Centre de Recherche Saint-Antoine (CRSA), 75012 Paris, France

[$]Corresponding authors: danielle.monniaux@inra.fr; rozenn.dalbies-tran@inra.fr

Funding

This work was supported by grants from France via the "Agence Nationale pour la Recherche" (http://www.agence-nationalerecherche.fr/) (ANR-12-BSV1-0034-02, AMHAROC). Anthony Estienne was supported by a French Fellowship from the Région Centre and INRA.

Acknowledgements

The authors acknowledge Damien Capo, Olivier Lasserre and the "ruminant" team of the "Unité Expérimentale de Physiologie Animale de l'Orfrasière" (UEPAO) for animal management and participation in the experimental design, Ramon Rubio (SIO ADM) for the gift of sesame oil used to dilute testosterone propionate before injections to ewes, Jean-Luc Touzé for ultrasonography scanning of lamb ovaries and Dominique Gennetay for her technical participation in hormonal assays. We acknowledge also the team of the "Chirurgie et Imagerie pour la Recherche et l'Enseignement" (CIRE) platform, particularly Gilles Gomot, Dominique Girardeau, Emilie Bled for abdominal magnetic resonance imaging analysis of sheep, and Jean-Philippe Dubois for animal slaughtering. The authors thank Julien Sarry for technical assistance in RNA library preparation, the staff of the GeT-Genotoul genomic platform (http://get/genotoul.fr) for RNA sequencing, and Sarah Maman of the INRA Sigenae bioinformatics team for Galaxy support. We address special thanks to Kim-Anh le Cao and Sebastien Dejean for mixOmics training. We are also very grateful to Frédérique Robin and Frédérique Clément for their help in statistical analyses of endocrine data and their invaluable inputs in writing the manuscript.

Abstract

In mammalian ovaries, the theca layers of growing follicles are critical for maintaining their structural integrity and supporting androgen synthesis. Through combining the postnatal monitoring of ovaries by abdominal magnetic resonance imaging, endocrine profiling, hormonal analysis of the follicular fluid of growing follicles, and transcriptomic analysis of follicular theca cells, we provide evidence that the exposure of ovine fetuses to testosterone excess activates postnatal follicular growth and strongly affects the functions of follicular theca in adulthood. Prenatal exposure to testosterone impaired androgen synthesis in the small antral follicles of adults and affected the expression in their theca cells of a wide array of genes encoding extracellular matrix components, their membrane receptors and signaling pathways. Most expression changes were uncorrelated with the concentrations of gonadotropins, steroids and anti-Müllerian hormone in the recent hormonal environment of theca cells, suggesting that these changes rather result from the long-term developmental effects of testosterone on theca cell precursors in fetal ovaries. Disruptions of the extracellular matrix structure and signaling in the follicular theca and ovarian cortex can explain the acceleration of follicle growth through altering the stiffness of ovarian tissue. We propose that these mechanisms participate in the etiology of the polycystic ovarian syndrome, a major reproductive pathology in woman.

Key Words

PCOS, collagen, SMOC, fibrillin, AMH, MRI, RNA sequencing, sheep

Abbreviations

AMH	Anti-Müllerian hormone
DEGs	Differentially expressed genes
ECM	Extracellular matrix
ELISA	Enzyme-linked immunosorbent assay
FSH	Follicle stimulating hormone
GO	Gene ontology
GnRH	Gonadotropin-releasing hormone
IPA	Ingenuity pathway analysis
LH	Luteinizing hormone
MRI	Magnetic resonance imaging
PCOS	Polycystic ovarian syndrome
RT-qPCR	Real-time quantitative PCR
sPLS	Sparse partial least squares

Introduction

Prenatal exposure to excess steroids or endocrine-disrupting compounds can lead to reproductive pathologies in adulthood. In humans, the polycystic ovarian syndrome (PCOS), involving oligo/anovulation, polycystic ovaries, hyperandrogenism and insulin resistance, is assumed to have different genetic and/or endocrine causes [1-3]. One of them is the high concentration of maternal serum testosterone affecting the fetuses during pregnancy [4-6]. The current assumption is that the hyperandrogenic intra-uterine environment could program the genes involved in ovarian steroidogenesis, insulin metabolism, gonadotropin secretion and ovarian follicle development, resulting in the development of PCOS in adult life [7].

Animal models of PCOS have been previously established by exposure to androgens in early life in mice, rats, primates and sheep. Sheep offer the advantage that their reproductive and metabolic developmental trajectory follows a similar time line as in humans, with ovarian follicle formation, hypothalamus and pancreas functional differentiation occurring during pregnancy [8]. From a practical perspective, sheep are easy to raise as domestic animals, and their large body size permits both the performance of endocrine profiling and the monitoring of ovarian follicular development by ultrasonography. In sheep, prenatal exposure to testosterone excess leads to reproductive failure in adult ewes [9, 10], resulting from the combination of neuroendocrine, metabolic and ovarian defects recapitulating those encountered in women with PCOS [8, 11]. The prenatally androgenized ewes experience a progressive deterioration of their reproductive axis after birth. The reproductive troubles include disrupted neuroendocrine feedback mechanisms, increased pituitary sensitivity to gonadotropin-releasing hormone (GnRH), luteinizing hormone (LH) excess and multifollicular ovarian morphology, culminating in anovulation during their second breeding season. The disruptions in the development of antral follicles and ovulation are likely the consequence of abnormal secretion of gonadotropins associated with the development of metabolic defects such as insulin resistance.

Prenatal testosterone excess enhances the activation of primordial follicles and early follicular development in fetal as well as postnatal sheep ovaries [12-14], yet the mechanisms underlying the short- and long-term acceleration of these processes remain unknown. It is very unlikely that the activation of early follicle development is caused by endocrine disruption, since the initiation of follicle growth is essentially triggered by local ovarian factors [15]. When ewes are treated with testosterone between 30 and 90 days of pregnancy, their fetuses are exposed to steroid excess during a period encompassing ovarian development and follicle formation [16, 17]. During the testosterone treatment of gestating ewes, the levels of testosterone in fetuses are increased, as are those of estradiol and estrone stemming from the aromatization of testosterone [18]. As the half-life of testosterone propionate is only 0.8 days [19], all steroids return to normal levels in the female fetuses shortly after stopping the treatment. Therefore abnormally high steroid levels cannot be directly involved in the activation of primordial follicles, which occurs from day 100 of pregnancy onwards in the fetal ovary [16]. Interestingly, the receptors to androgens (AR) and estrogens (ESR1 and ESR2) are all expressed in the ovarian cortical stroma of the fetal sheep during the treatment period [20]. Altogether, these observations suggest that accelerated follicle activation and growth following prenatal testosterone exposure might result from long-term developmental effects of steroids on cortical cells in the fetal ovary.

During follicular development beyond the primary follicle stage, theca cells are recruited from surrounding ovarian cortical cells [21-23]. After prenatal exposure to a testosterone excess, reduced expression of key genes involved in ovarian steroid synthesis such as *STAR*, *CYP11A1*, *CYP17A1*, and *LHCGR* has been

observed in the whole fetal ovary at day 90 of gestation [24]. Immunohistochemistry experiments have revealed a reduced thecal CYP17A1 expression in adult ovaries after prenatal testosterone exposure [25], and the thecal androgen production seems to be affected differentially according to the size of antral follicles [26]. Altogether, these results suggest that the fetal irreversible changes of ovarian cortical cells, particularly theca cell precursors, could have long-term consequences on the steroidogenesis of theca cells in the growing follicles of adult ovaries. Moreover, thecal steroidogenesis in adulthood is likely stimulated by the high LH blood levels resulting from the exposure of hypothalamus to testosterone during fetal life [27]. Whether other thecal functions are affected by the prenatal testosterone treatment and what mechanisms underlie these changes remain unknown.

In this study, we aimed to understand the mechanism by which prenatal exposure of ovaries to testosterone excess activates the development of growing follicles after birth. Hypothesizing a role of fetal irreversible changes of follicular theca cell precursors in this process, we intended to establish (1) the consequences of prenatal exposure to testosterone on the gene expression profile of theca cells in adulthood (2) the extent to which the most recent hormonal environment of follicles has influenced gene expression in theca cells. To answer these questions, we have followed postnatal ovarian and endocrine changes in sheep after prenatal exposure to testosterone excess, established the transcriptome of theca cells in growing follicles of adult ovaries, and studied the possible relationships between the recent hormonal environment of follicles and gene expression in their theca cells.

Materials and methods

Animals and experimental design

Experiments were conducted on Ile-de-France sheep (*Ovis aries*) maintained under normal husbandry at the research station of the Institut National de la Recherche Agronomique in Nouzilly (Unité Expérimentale PAO no. 297, EU0028). All procedures were approved by the French Agricultural and Scientific Research Government Committee (Approval number E37-175-2) and the Val de Loire ethics committee for animal experimentation (Referral 2012-12-21, n°19), in accordance with the guidelines for Care and Use of Agricultural Animals in Agricultural Research and Teaching.

A prolific strain of Ile-de-France sheep was used in this study. Adult ewes were mated with rams in April (spring season). Between 30 and 90 days of gestation, ewes were treated twice a week by intra-muscular injections of 100 mg testosterone propionate (AMSBIO, UK) diluted in sesame oil (n=17 testosterone-treated ewes), or sesame oil (SIO ADM, France) used as a diluent (n=17 control ewes), as described previously [28]. As expected, the testosterone concentrations were high in the plasma of testosterone-treated ewes at 62 and 90 days of gestation, but low and similar to those of control ewes at 140 days of gestation (Fig. S1A). At parturition (in September, autumn season), 53% of the ewes gave birth to dizygotic twins (resulting from the fertilization of double ovulations). The mean offspring per ewe was similar between groups (Fig. S1B). The total numbers of male and female lambs born alive to the testosterone-treated and control ewes were not significantly different (Fig. S1C). Immediately after birth, the lambs were separated from their mothers and fed with artificial milk. Lambs were weighed at birth and their degree of masculinization was assessed by their ano-genital ratio (anal-genital distance/ umbilical-anal distance). The genetic sex of lambs was determined from a blood sample by PCR analysis [29] in order to keep only female lambs. The female lambs born to testosterone-treated (group T lambs) and control ewes (group C lambs) were kept in close pens inside the same livestock building, to minimize any potential variation due to the external environment. Animals were weighed every 2 weeks from birth to 26 weeks of age, then monthly

afterwards. At 52 weeks of age, the thickness of their dorsal skin, fat and muscle was assessed by ultrasound analysis. Blood samples were collected at each weighing time for hormonal monitoring, and plasmas were stored at -20°C until anti-Müllerian hormone (AMH), testosterone, follicle stimulating hormone (FSH) and LH assays were performed. To detect estrous cycles at the first breeding season (autumn season), additional blood samples were taken weekly during 5 consecutive weeks when animals were 52 and 60 weeks old, and plasmas were stored until progesterone assay. To find out information on follicular counts, the animals underwent abdominal magnetic resonance imaging (MRI) analysis at 8, 18, 26 and 52 weeks of age. They were slaughtered at 67 weeks of age in a local abattoir. At the end of the experiment, the animals received a norgestomet subcutaneous implant (Crestar, France) for 10 days and were slaughtered 7 days after removal of the implant, during the luteal phase of the synchronized estrous cycle.

Collection of ovarian cells and in vitro oocyte maturation

The ovaries were collected immediately after slaughtering. An ovarian fragment containing follicles smaller than 1 mm in diameter was fixed in Bouin fixative for further immunohistochemistry experiments, and then the ovaries were dissected to isolate all the antral follicles equal to or larger than 1 mm in diameter. Follicles were allocated to 3 size classes: 1–3 mm (including 1 and 3 mm diameter follicles), 3–5 mm (including 5 mm diameter follicles) and > 5 mm in diameter. Using a lancet, all dissected follicles were opened under a stereomicroscope in order to collect the oocyte and follicular cells. For seven animals (4 in group C, 3 in group T) oocyte chromatin was analyzed at this stage. For nine animals (5 in group C, 4 in group T), cumulus enclosed oocytes were incubated for 22 to 24 h at 38.5°C in a 80 µl drop of TCM-199 medium (Sigma) supplemented with 10 ng/ml EGF (Epidermal Growth Factor, Sigma), 100 µM cysteamine (Sigma) and gentamicin under mineral oil. Then oocytes were denuded by pipetting, fixed in 4% paraformaldehyde, rinsed in phosphate buffered saline, and mounted in Hoechst 33342-containing mowiol. After oocyte collection, granulosa cells and follicular fluid were recovered from each follicle as described [30], and fragments of theca were finely dissected and washed before storage. For 1-3 mm diameter follicles, follicular fluid, granulosa cells and theca fragments were pooled separately (2 to 5 pools of each sample type from 8-10 follicles per animal). Samples were stored at −80°C for further analysis.

Abdominal MRI analysis

A 3 Teslas (T) MRI scanner (Siemens Magnetom® Verio, Erlangen, Germany) was used to analyze the abdominal cavity of anaesthetized animals. We used a 32 phased array torso coil (split into 2, 16 anterior and 16 posterior). Multiplanar, T_2-weighted 2-dimensional Turbo Spin-Echo (TSE) imaging was performed in both axial and coronal planes. The MRI parameters for these anatomical images were set as follows: Repetition Time (TR)=12930 ms, Echo Time (TE)=88 ms, Field-of-View (FOV)=250x250 mm², pixel matrix size=640x640, resulting in an in-plane resolution of 0.39x0.39 mm² with a slice thickness of 1.5 mm and 40 joint slices. The number of averages were set to 4, the flip angle to 150° and an integrated Parallel Acquisition Technique (iPAT) of 2 was used making a total acquisition time of 14 min and 54 sec for each plane. The bandwidth was 230 Hz/Px. To obtain a good overview of each ovary and determine the number of follicles over 1 mm it contains, the two separate acquisition planes were displayed. The images of 10 successive slices (chosen as axial and/or coronal, depending on image sharpness) covering the whole ovary were then analyzed. The antral follicles appeared as white ovoid structures on the images (Fig. 1). A linear relationship was found between the numbers of 1-3 mm follicles counted by either MRI or ovarian ultrasonography at 26 weeks of age ($r=0.68$, $p < 0.01$, $n=16$). The slope of the regression line was

1.44, indicating that MRI analysis was more efficient than ultrasonography to detect the small antral follicles < 2 mm in diameter.

Hormonal assays

The AMH concentrations in plasma and follicular fluids were determined using the AMH Gen II ELISA kit (Beckman Coulter), as previously described [30], on 50 µl aliquots of undiluted plasma and follicular fluid diluted to 1/1000 for follicles < 5 mm, and 1/100 or 1/10 for follicles > 5 mm in diameter. The limit of detection of the assay was 20 pg/ml and the intra-assay coefficients of variation (s.e.m./mean) were 11.8% and 3.6%, for quality control plasma samples containing 33 pg/ml and 125 pg/ml AMH, respectively. The testosterone concentrations in plasma and follicular fluids were determined using a radioimmunoassay developed in our laboratory, as previously described [31], on 10 µl aliquots of undiluted plasma and follicular fluid diluted to 1/10. The limit of detection of the assay was 0.06 ng/ml and the intra-assay coefficients of variation were 7.6% and 4.1% for quality control samples containing 0.5 ng/ml and 4 ng/ml testosterone, respectively. The progesterone concentrations in plasma and follicular fluids were determined using an enzyme-linked immunosorbent assay (ELISA) developed in our laboratory, as previously described [32], on 10 µl aliquots of undiluted plasma and follicular fluid diluted to 1/10. The limit of detection of the assay was 0.4 ng/ml and the intra-assay coefficient of variation was 6.6% for quality control plasma samples containing 1.5 ng/ml progesterone. The estradiol concentration in follicular fluids was determined using the E2-EASIA immunoassay kit (DIAsource), as previously described [33], on 25 µl aliquots of follicular fluid diluted to 1/10 and 1/100 for follicles < 5 mm and > 5 mm in diameter, respectively. The limit of detection of the assay was 3 pg/ml and the intra-assay coefficient of variation was lower than 7% for quality control follicular fluid samples with concentrations in the range of 3 pg/ml to 100 pg/ml. The FSH concentration in plasma was determined using an ELISA developed in our laboratory, on 20 µl aliquots of undiluted plasma, as previously described [34]. The limit of detection of the assay was 0.4 ng/ml. The intra-assay coefficient of variation was 1.4% for quality control plasma samples containing 3 ng/ml FSH. The LH concentration in plasma was determined using an ELISA developed in our laboratory, on 20 µl aliquots of undiluted plasma, as previously described [34]. The limit of detection of the assay was 0.1 ng/ml. The intra-assay coefficient of variation was 1.3% for quality control plasma samples containing 0.6 ng/ml LH.

RNA extraction and assessment of quantity, purity and quality

Total RNA was extracted from ovarian cell samples with a Nucleospin RNA II kit (Macherey-Nagel) according to the protocol of the manufacturer and including a DNAse1 treatment step. The yield of RNA was quantified by absorbance using a NanoDrop® ND-8000. For RT-qPCR experiment, 34 samples corresponding to 14 animals (7 in each group C and T) were analyzed. Within each group, 2 animals and 5 animals provided 1 pool and 3 pools of 8-10 follicles respectively. For RNA sequencing, the quality of the RNA extracted from theca cells was assessed using a Fragment Analyzer™ (Advanced Analytical Technologies). Only RNA samples whose RNA Quality Number ranged from 7.1 to 8.5 were selected for the libraries sequencing (group C, n=5 and group T, n=5).

Library preparation and high-throughput RNA sequencing

All RNA sequencing libraries were constructed from 1 µg of total RNA and sequenced using Illumina TruSeq RNA Sample Prep (Illumina) as already described [35]. Sequencing was performed on an Illumina HiSeq 3000 apparatus using the Illumina TruSeq Standard mRNA kit v2 to obtain paired-end reads (2 x 150 bp).

Bioinformatics analysis

We applied the entire bioinformatic pipeline already used and described [35]. Briefly, after quality control and E. coli, Phi phage or yeast sequences contamination removal, the FastQ files were processed using the local instance of Galaxy (https://galaxyproject.org) on a local bioinformatics platform (http://sigenae-workbench.toulouse.inra.fr/). The FastQ files and metadata were submitted to the Sequence Read Archive (SRA) at NCBI (SRP 189299). The paired reads were mapped against the ovine genome assembly (Oar_v3.1.84) using STAR2 (STAR_2.4.0i, Galaxy tool v2.0). Based on the Ensembl annotation file (Ovis_aries.Oar_V3.1.84), read counting for the annotated genes of each sample was done using the Cufflink software. The ten files with raw counting were merged to prepare a final count file in RPKM (reads per kilobase of transcript per million fragments mapped) for statistical analysis of differential gene expression.

Differentially Expressed Gene analysis

SARTools R package 1.3.2 [36] was used for the descriptive and diagnostic analyses, allowing us to discard 2 disagreeing samples. The raw counts from the remaining 8 samples were normalized for library size. A generalized linear model was fitted on the normalized raw count data using the DESeq2 R package version 1.12.3 [37] to identify the differentially expressed genes (DEGs) between group C (n=4) and group T (n=4). The raw P-values were adjusted for multiple testing using the Benjamini-Hochberg procedure to control for the false discovery rate (FDR) [38]. Genes with an adjusted P-value lower than 0.05 (FDR < 5%) were considered as DEGs and selected for subsequent analyses. The Ensembl_ID was converted to official gene name according to the HUGO Gene Nomenclature Committee (HGNC) with BioMart [39]. For unknown genes without HUGO gene name, a manual annotation has been attempted through NCBI's BLAST (https://blast.ncbi.nlm.nih.gov) using the ovine genome assembly Oar_v4.0 or through comparative genomics using Genomicus (http://www.genomicus.biologie.ens.fr) [40]. Thus, among the 657 DEGs, 19 Ensembl_IDs were still unannotated, 9 were long non-coding RNAs and 38 were LOC genes (genes with published symbol not yet available).

Gene Ontology (GO) enrichment analysis

The list of DEGs with automatically or manually obtained HUGO gene names was analyzed with the Enrichr web-based tool (http://amp.pharm.mssm.edu/Enrichr) [41, 42]. A total of 626 genes were recognized and submitted to a GO terms enrichment analysis. The 2018 GO update was used for biological processes, molecular functions and cellular components terms. Enrichr computes different enrichment result scores based on standard Fisher's exact test (F-test), providing (1) a P-value, (2) an adjusted P-value using the Benjamini-Hochberg procedure, (3) a correction to the F-test delivering a Z-score (rank score) and (4) a combined score, calculated by multiplying the log of the F-test's P-value by the Z-score. Top 5 enriched terms were considered and ranked using the combined score (Table 1).

Ingenuity pathway analysis

A thorough analysis was run with Ingenuity Pathway Analysis (http://www.ingenuity.com, IPA) system, which is a resource based on an expert manual annotation. The DEG dataset containing official HUGO gene name, log2 Fold change and adjusted P-value was uploaded in IPA. Known canonical pathways enriched with genes of interest were obtained from the DEG list (n=586 genes spotted by IPA). Significant values for canonical pathways were calculated by using a right-tailed Fisher's exact test. A cut-off P-value of 0.05 was used as threshold. Network analysis was performed, allowing direct and undirected interactions between DEGs, to infer relevant networks. Finally, the "overlay" tool was used to design and visualize the pathway and network results.

MixOmics analysis

The mixOmics project (www.mixomics.org) proposes a large range of multivariate statistical methods for the exploration and integration of various high dimensional biological datasets. Here, the associations between transcriptomic and phenotypic data sets measured on the same ewes (n=4 in group C and n=4 in group T) were investigated with the mixOmics R package version 6.32 [43, 44]. The first dataset was made up of the normalized counts for the 657 DEGs. The second dataset was made up of 1) the concentration of 4 hormones (AMH, testosterone, estradiol and progesterone) in the follicular fluid of 1-3 mm diameter follicles at 67 weeks of age (at slaughtering) and 2) the mean plasma concentration at 59, 62 and 67 weeks of age for AMH, FSH, LH and testosterone. Parsimonious statistical methods, such as sparse Partial Least Squares (sPLS) analysis, allowed variable selection and calculated association between datasets. Sparse PLS in canonical mode maximized the covariance between components corresponding to linear combinations of selected relevant variables from both data sets. First, the *tune.spls* function was used to determine optimal values for the sparse parameters (i.e. number of components, n parameter and number of variables to keep, k parameter), which are data driven. Then, the sPLS analysis by itself was run using the optimal number of components (set to 6), and with the number of DEGs per component set at 50 (k parameter from *tune.spls* function). Relationships between variables were visualized with a correlation circle plot, which represents the correlation between the initial data and its associated components (*PlotVar* function). The relevant network of positive and negative covariances was obtained from network function and used for graphical outputs. To draw the network, data were exported to Cytoscape 3.7.1 (https://cytoscape.org/) with an absolute value threshold for the correlation superior to 0.7.

Real-time quantitative PCR (RT-qPCR) analysis

One µg of total RNA from ovarian cell samples was used for reverse transcription using anchored oligo-dT (T22V) primer and Superscript II reverse transcriptase (Invitrogen, France). Primer design using Beacon designer 8.20 (Premier Biosoft), SYBR green real-time PCR cycling conditions using QuantStudio 6 Flex Real-Time PCR system (ThermoFisher Scientific) and amplification efficiency calculation were performed as already described [35]. Primer sequences, amplicon length and amplification efficiency are listed in Table S1. RNA transcript abundance was quantified using the ΔΔCt method [45] with the geometric mean expression of *GAPDH*, *RPL19* and *SDHA* as internal reference and a pool of all cDNA samples as calibrator. The three reference genes were validated by the Bestkeeper algorithm [46].

Immunohistochemistry

Ovarian fragments were embedded in paraffin and serially sectioned at a thickness of 7 µm with a microtome. Immunohistochemistry experiments were run on ovarian sections as previously described [47]. The mouse monoclonal anti-COL7A1 antibody LH7.2 (Genetex) and the rabbit polyclonal anti-SMOC2 antibody orb101348 (Biorbyt) were used as primary antibodies suitable for the ovine species, after dilution 1/200 and 1/40 respectively. The secondary antibody was the biotinylated anti-mouse IgG/anti-rabbit IgG (Vector Laboratories) diluted 1/800. The avidin-peroxidase conjugate from Vectastain Elite ABC kit (Vector Laboratories) was used for signal amplification before staining revelation. Negative control sections involved omission of the primary antibody from the procedure.

Statistical analysis of phenotypical, ovarian and hormonal data

Comparisons between testosterone-exposed and control female lambs were made on the animals which were available and kept healthy up to slaughtering at 67 weeks of age. Each group of eight animals contained a couple of dizygotic twins, which experienced the same in utero environment. We have checked that removing one animal

(chosen at random) of each couple did not change the results of statistical analyses and therefore we have considered that all the animals were independent individuals. All data are presented as mean ± s.e.m. Statistical analyses were performed using the GraphPad Prism 7 Software. Percentages were compared using Chi-square analysis. The comparison of two means between groups were done using t test, with Welch's correction when variances were heterogeneous. For comparisons of intra-follicular hormonal concentrations between the different size classes of follicles within each group, data were analyzed using Kruskal-Wallis test. For the study of plasma hormone concentrations, two types of comparisons were performed. Mann-Whitney test was used to compare hormone levels between groups. Paired Wilcoxon signed rank test was used to study the chronology of the first AMH and FSH peak within each group. From birth, the AMH and FSH time series were characterized by steadily increasing values up to a maximum value, which was identified as the first peak. We retrieved the corresponding time index that was subjected to the statistical test. Classical methods used to study time series such as cross-correlations were not applicable, since, as expected from their non-monotonic pattern, the hormonal series are not stationary (Dickey-Fuller, Augmented Dickey-Fuller and Philipps-Perrons tests) [48]. For all analyses, a probability lower than 0.05 was required for significance, but probabilities up to 0.10 are indicated between brackets in the Figures.

Results

Postnatal developmental phenotype of the prenatally androgenized sheep

Testosterone-exposed female lambs (group T, n=12), born to eight ewes treated with intramuscular injections of testosterone propionate between 30 and 90 days of pregnancy, have been compared to control lambs (group C, n=10) born to eight ewes treated with diluent alone. At birth (in September, autumn season), lambs had similar weights in groups C and T (Fig. S2A). Female lambs of group T exhibited an ano-genital ratio similar to that of the male lambs (Fig. S2B), confirming their masculinization. Postnatal growth of the female animals was similar in groups C and T, and the thickness of their dorsal skin, fat and muscle at 1 year of age showed no difference between groups (Fig. S2C and S2D). As sheep are seasonal breeders responsive to photoperiod changes, we studied the presence of estrous cycles in adults from the beginning of their first breeding season, when they had reached the age of 1 year. At this time (autumn season), the percentage of animals with defects in estrous cycles (short cycles or absence of cycles) was higher in group T (75.0%) than in group C (22.2%) (Table S2). Eight out of the twelve female animals of group T exhibited abdomen abnormalities, consisting of uterine cysts, pyometer and/or abnormal septa in the bladder, detected by abdominal MRI on anesthetized animals (Fig. S3) or discovered after animal slaughtering. Five of these animals had to be slaughtered before 67 weeks of age, in accordance with ethical concerns.

Populations of antral follicles in the postnatal ovaries

From abdominal MRI analysis performed on eight animals in each group at 8, 18, 26 weeks of age and in adulthood (at 52 weeks of age), the numbers and sizes of antral follicles visualized on the ovaries were quite variable between animals of similar age within each treatment group (Fig. 1 and S4). Three follicular classes were defined (1–3 mm (including 1 and 3 mm diameter follicles) ; 3–5 mm (including 5 mm diameter follicles) ; > 5 mm), corresponding to follicle growth, selection and dominance stages, respectively [15]. The number of 1-3 mm diameter follicles decreased between 18 and 26 weeks of age in both groups, but was clearly higher in animals of group T at 18 and 26 weeks of age, compared to animals of similar ages in group C (Fig. 2).

Postnatal endocrine changes

To characterize the postnatal secretion of ovarian hormones and gonadotropins, we studied the changes in AMH and testosterone (known to be secreted by the granulosa and theca cells of growing follicles, respectively) concentrations in the plasma of eight animals in each group, concomitantly with the changes in FSH and LH plasma concentrations.

In both groups, AMH concentrations were undetectable at birth, then increased and peaked synchronously at 8 weeks of age. The average AMH concentrations during the periods 14-26 weeks and 30-51 weeks were higher in group T, compared to group C, but the most pronounced difference in AMH concentrations occurred during weeks 8-12 (Fig. 3a and 3b). AMH has been shown to be an endocrine marker of the population of small antral follicles in sheep [49, 50]. In consistency with these observations, we found that the number of 1-3 mm diameter follicles at 8 weeks of age was positively correlated with the maximum AMH concentration ($r=0.77$, $p < 0.01$) and with the average AMH concentration during the period 0-12 weeks ($r=0.71$, $p < 0.01$). Also, the number of 1-3 mm diameter follicles at 18 and 26 weeks of age was positively correlated with the average AMH concentration during the period 14-51 weeks ($r=0.61$ and $r=0.63$, respectively, $p < 0.05$). In both groups, testosterone concentrations were undetectable from birth to 4 weeks, then displayed similar variation profiles. The testosterone concentrations at 8 and 26 weeks of age and the average testosterone concentration during the period 0-12 weeks were lower in group T, compared to group C (Fig. 3c and 3d).

In both groups, FSH concentrations were undetectable at birth but increased thereafter. The first FSH peak occurred 2 weeks earlier, on average, in group T compared to group C (Fig. 4a). In relationship with this lag, FSH concentrations were higher at 2 weeks of age and lower at 6 weeks of age in group T, compared to group C. FSH concentration was also lower at 22 weeks of age in group T, but the average FSH concentrations did not differ significantly between groups during any time period (Fig. 4b). In both groups, the first FSH peak preceded the first AMH peak. There was an average lag of 2 weeks between the FSH and AMH peaks for the group C and 4 weeks for the group T. In both groups, LH concentrations were undetectable at birth, then displayed similar variation profiles (Fig. 4c). The average LH concentrations were higher during the period 55-67 weeks in group T, compared to group C (Fig. 4d).

Main features of antral follicles and oocytes at animal slaughtering

When dissecting the ovarian follicles of the slaughtered animals (group C, n=9, and group T, n=7), the ovarian tissue of group T was noticed to be particularly soft and sticky, indicating a weak tissue stiffness. The total number of dissected follicles larger than or equal to 1 mm in diameter was higher in group T than in group C (Fig. 5a). In both groups, the intra-follicular concentrations of estradiol and progesterone increased with follicular diameter (Fig. 5d and 5e). Conversely, the intra-follicular concentrations of AMH decreased (Fig. 5b), while the decrease in testosterone concentrations was significant only in group T (Fig. 5c). The 1-3 mm diameter follicles displayed lower intra-follicular concentrations of testosterone and higher concentrations of progesterone in group T than in group C (Fig. 5c and 5e).

Most oocytes from follicles larger than 1 mm in diameter were at the expected germinal vesicle stage in both experimental groups. The proportion of oocytes able to resume meiosis up to the metaphase II stage after *in vitro* maturation was not different between groups (53 % (n=38) *vs*. 50 % (n=48), group C vs. group T).

Gene expression in the theca of 1-3 mm diameter follicles

The differences found between experimental groups for testosterone and progesterone concentrations in the 1-3 mm diameter follicles suggested functional differences at the level of theca cells. RNA sequencing analysis of theca samples of 1-3 mm diameter follicles from four animals in each group has revealed 657 genes with differentially accumulated mRNA between groups (Fig. S5 and Table S3). A gene ontology analysis through the enrichment analysis tool Enrichr has shown that the biological processes controlled by the DEGs mainly concern the organization of extracellular matrix (ECM) ; the pathways found to be relevant are mostly those of collagens, ECM-receptor interaction (focal adhesion, integrins) and several growth factors (TGFβ, IGF) (Table 1). Using the Ingenuity Pathway Analysis software, we have built a network of 29 DEGs, including genes encoding matrix components (different collagen chains, thrombospondin-1) together with their membrane receptors and co-factors (integrins, tetraspanins), connected with signaling pathways regulating cell apoptosis and proliferation (JNK1/2 and PI3K/AKT) (Fig. 6).

To validate the differences in gene expression, RT-qPCR was run on samples of follicular theca retrieved from seven animals per group. Twelve genes were selected for both their high expression level and their importance in ECM organization or intercellular junctions (Table 2). A differential expression between groups was confirmed for nine out of these genes (5 out of 7, and 4 out of 5 genes, respectively with a higher and lower expression in group T, compared to group C, Table 2). When RT-qPCR analyses were performed on granulosa cell samples retrieved from the same follicles than the analyzed theca samples, no similar differences between groups were observed, except for *FBN3* (data not shown). This highlights a high tissue specificity of the impact of prenatal excess testosterone exposure on the expression of these genes.

To establish whether mRNA changes could be associated with similar changes in protein amounts in the theca of antral follicles, immunohistochemistry experiments were carried out on ovarian sections of five animals from both experimental groups. Two factors involved in ECM organization, COL7A1 and SMOC2, were chosen for these experiments, because they exhibited respectively a lower and a higher mRNA expression level in group T by both RNA sequencing and RT-qPCR analyses (Table 2), and antibodies suitable for the ovine species were available. There was a lower COL7A1 (Fig. 7, panels a vs. b, and e vs. f) and higher SMOC2 (Fig. 7, panels g vs. h, and k vs. l) immunostaining intensity in the theca of small antral follicles from group T, compared to group C, in agreement with the mRNA expression level (Table 2). In the ovarian cortex, COL7A1 immunostaining intensity was lower in group T, compared to group C (Fig. 7, panels c vs. d), whereas SMOC2 immunostaining was similar between groups (Fig. 7, panels i vs. j).

Relationships between gene expression in follicular theca and the hormonal environment of follicles

In small antral follicles, theca cells are known to be the direct targets of LH, steroids and AMH [21, 22, 51, 52], whereas FSH, acting on granulosa cells, also modulates theca cell functions through paracrine mechanisms of regulation [2, 53, 54]. Indeed, in this study, the gene expression in follicular theca could have been affected by the most recent hormonal environment of follicles. To test this hypothesis, we looked at the relationships between the mRNA levels of the DEGs in the theca of 1-3 mm diameter follicles, the intra-follicular concentrations of AMH, testosterone, estradiol and progesterone in the 1-3 mm diameter follicles, and the mean plasma concentrations of AMH, testosterone, FSH and LH during the 8 weeks preceding slaughtering (from 59 to 67 weeks of age).

The correlation circle plots from sPLS analysis in the canonical mode between DEGs mRNA levels and hormonal measures have shown that the mRNA levels of several DEGs were closely correlated (positively or negatively) with LH plasma or/and progesterone intra-follicular concentrations, which in turn were found

negatively related to FSH plasma or/and testosterone intra-follicular concentrations (Fig. S6). When considering a threshold of 0.7 for the association, the mRNA levels of 124 DEGs (only 19% of the total DEGs) were found correlated, positively or negatively, with at least one hormonal measure (Fig. 8). Hence, in theca cells, the expression of only a minor part of the DEGs appeared to be modulated by gonadotropins and intra-follicular hormones.

As shown above, LH plasma concentrations during the 8 weeks preceding slaughtering, and progesterone intra-follicular concentrations at slaughtering, were both higher in group T, compared to group C (Figs. 4 and 5). Thus, the DEGs whose mRNA levels were correlated with these hormonal measures could be proposed as potential target genes of LH and/or progesterone. When considering a threshold of 0.7 for the association, the network of positive and negative covariances between DEGs mRNA levels and hormonal measures have identified 36 and 30 known DEGs, whose mRNA levels were respectively positively and negatively correlated with LH plasma concentrations (Fig. 8). These potential LH targets include a few genes encoding ECM components (*COL16A1*, *GPC5*, *SDC3*, *SMOC2*), some of them directly involved in TGFβ processing and secretion (*LTBP1*, *LTBP4*), and components or regulators of the cytoskeleton (*ARHGAP45*, *CTNNA2*, *EML5*, *INF2*, *KIF12*, *KIF21A*, *PHLDB1*, *SLMAP*, *TPM1*, *VCL*). Among the 66 DEGs whose mRNA levels were highly correlated with LH plasma concentrations, 42 (63.6%) exhibited also high correlations with progesterone intra-follicular concentrations. For these latter genes, positive (and negative, respectively) correlations were found between the mRNA levels of 19 DEGs (and 23 DEGs, respectively), and both LH plasma and progesterone intra-follicular concentrations.

As shown above, testosterone intra-follicular concentrations were lower in the 1-3 mm diameter follicles from group T, compared to group C (Fig. 5). Among the 27 DEGs whose mRNA levels were highly correlated with testosterone intra-follicular concentrations, only one (*THBS1*, encoding Thrombospondin-1) encoded an ECM component.

Discussion

In this study, we have shown for the first time that the exposure of ovine fetuses to testosterone excess has affected the expression in adult ovaries of a wide array of genes encoding ECM components and their signaling pathways in the theca of small antral follicles. Part of the observed expressional changes might have occurred in response to enhanced LH blood levels in adulthood, yet most of them could result from direct developmental effects of testosterone on the fetal ovary. We propose that disruptions of the ECM structure and signaling in the follicular theca and ovarian cortex can explain the acceleration of follicle activation and growth observed on the long term in the prenatally androgenized ovaries.

Testosterone, when administrated to sheep fetuses between 30 and 90 days of gestation, exerts pleiotropic effects on various organs with important consequences on the reproductive function in adults. In this study, testosterone has induced the masculinization of female lambs at birth, affected the follicular development and, at the first breeding season of animals, increased LH endocrine levels and altered estrous cycles. These results confirm the impact of testosterone previously shown on the tubular and external genitalia [55] and the hypothalamus-pituitary-ovary axis of fetuses [8]. From our results, the prenatally androgenized lambs did not differ from control lambs as far as their postnatal body growth and dorsal skin, fat and muscle thicknesses are concerned. However, we have not investigated the metabolic consequences of the testosterone treatment. The progressive

development of insulin resistance and visceral adiposity previously reported for prenatally androgenized lambs [56-59] may have also participated in modulating the reproductive function [2, 60].

Our results confirm that the prenatal exposure of fetuses to testosterone excess has activated postnatal follicular growth in ovaries. To our knowledge, this is the first study using abdominal MRI analysis to count antral follicles in sheep ovaries *in vivo* and explore the consequences of fetal exposure to testosterone on follicular growth. Before one year of age, the number of small antral follicles in ovaries was higher in the prenatally androgenized lambs than in control lambs and, concomitantly, their AMH plasma levels were increased. It is now well established that AMH is an endocrine marker of this follicle subpopulation in sheep [49, 50], as in other mammals [61-63]. Hence, both follicle numbers in ovaries and AMH plasma concentration patterns indicate that *in utero* exposure of fetuses to testosterone has stimulated postnatal follicular growth. Even if gonadotropin supply is not essential for the growth of follicles up to the small antral follicle stage (about 2 mm in diameter in sheep), the preantral and small antral follicles contain FSH-responsive granulosa cells, and FSH is probably important for an optimal development [15, 64]. In this study, a postnatal FSH peak preceded the AMH peak in both groups, suggesting that FSH could have supported the first postnatal wave of follicular development, as previously suggested in ruminants [65]. However, the extension of the time interval between the FSH and AMH peaks in prenatally androgenized lambs (4 weeks), compared to control lambs (2 weeks), and the absence of any difference in FSH concentrations between groups, do not argue in favor of a possible role of FSH in activating follicular growth in the ovaries of prenatally androgenized lambs.

LH also is needed to support follicular development, since this gonadotropin stimulates progestogen and androgen production by the LH-responsive steroidogenic theca cells of the multilayered growing follicles [15, 21, 22]. From our results, during the first breeding season of animals, despite higher LH levels in the plasma of prenatally androgenized sheep, confirming previous observations [5, 66] and higher numbers of antral follicles in their ovaries, the testosterone plasma levels did not increase concomitantly. Moreover, in the prenatally androgenized animals compared to control, the testosterone concentrations in the follicular fluids of small antral follicles were even lower, and progesterone concentrations were higher. This latter result suggests that the biosynthesis of androgens from progestogens was disrupted in theca cells, possibly resulting from a decreased CYP17A1 expression, as previously shown by immunohistochemistry in the theca of prenatally androgenized sheep [25]. From our results, a tendency to a lower *CYP17A1* mRNA expression was observed in the theca of small antral follicles from prenatally androgenized sheep (data not shown). Altogether, these observations indicate that *in utero* testosterone treatment of fetuses has affected the steroidal function of theca cells in adults.

The theca layer of ovarian follicles is an envelope of connective tissue containing not only steroidogenic cells, but also fibroblasts, blood vessels and perivascular smooth muscle cells [21, 22]. The theca is thus critical for maintaining the structural integrity of the follicle. From our results, the exposure of ovine fetuses to testosterone had a strong impact on the expression of genes encoding factors involved in ECM organization and tissue architecture in the theca of small antral follicles of adults. The expression of different collagen chains was particularly affected by the testosterone treatment. For instance, the expression of *COL7A1* mRNA and its encoded protein, the collagen alpha-1(VII) chain, was severely decreased in the follicular theca of prenatally androgenized sheep. The homotrimer collagen VII forms anchoring fibrils, which bind collagen IV and laminin 332 in epithelial basement membranes and the α6β4 integrin in hemidesmosomes, thus maintaining epithelial-mesenchymal cohesion in tissues [67]. Mutations in *COL7A1* are known to be the cause of dystrophic epidermolysis bullosa, a

rare genetic skin disease in humans [68]. In the follicular theca of prenatally androgenized sheep, concomitantly to the lower expression of *COL7A1*, the expression of *TLL2*, encoding tolloid like 2, a proteinase involved in processing the C-terminal propeptide of collagen VII [69] was increased, as was the expression of *ITGA6*, encoding integrin subunit α6. Abnormal expression of these interacting factors could affect the epithelial basement membrane organization and adherence between cells. Moreover, in prenatally androgenized sheep, the low expression of *COL9A1* and *COL9A3*, encoding components of collagen IX involved in connective tissue cohesion [70], and the high expression of *COL6A6*, encoding a component of collagen VI involved in ECM structure and biomechanical properties [71] could participate in altering the tissue stiffness in follicular theca. None of these collagen genes have been found differentially expressed in bovine theca cells during follicular growth or atresia [72, 73], suggesting that the changes observed in the prenatally androgenized ovaries of sheep reflect a pathological, rather than a physiological process of follicular development. However, one may note that follicle development is not fully abnormal in prenatally androgenized sheep since their antral follicles can develop to a preovulatory size, synthesize estradiol like healthy mature follicles and shelter an oocyte able to resume meiosis up to the metaphase II stage after *in vitro* maturation.

Among the differences evidenced in the theca cell transcriptome following *in utero* testosterone treatment of sheep, some may have occurred in response to the elevated circulating LH levels and LH pulse frequency known to occur in the prenatally androgenized animals in adulthood [74]. From our results, strong correlations were observed between LH concentrations measured during the last weeks preceding animal slaughtering and the expression level of several genes, which appear to be potential LH targets. These targets include the collagen chain COL16A1, and non-collagen ECM components such as the matricellular protein SMOC2 (SPARC related modular calcium binding 2), whose expression in terms of both mRNA and the encoded protein was enhanced in the follicular theca of prenatally androgenized sheep, the cell surface proteoglycans GPC5 (glypican-5) and SDC3 (syndecan-3), and factors involved in TGFβ processing and secretion, or cytoskeleton regulation. In the theca cells of bovine follicles collected 21 hours after an exogenous GnRH-induced LH surge, more than 200 transcripts specifically regulated by LH have been identified [75]. In our study, among the 66 genes whose expression levels were correlated with plasma LH concentrations, only *TSPAN33* and *F5*, encoding respectively the transmembrane protein tetraspanin-33 and the coagulation factor V, belong to the list of LH target genes previously proposed [75], and among the 657 DEGs, only 8 genes (*GCLC*, *SLC35G1*, *ATF6*, *PHLDA1*, *TNNT1*, *TSPAN33*, *F5* and *COLEC11*) belong to this list. The discrepancies between these transcriptomes could be explained by differences in LH effect types (acute versus chronic) between studies. Indeed, in our study, part of the LH effects is not direct, but likely relayed by paracrine mechanisms of regulation. For instance, the 42 genes whose expression levels were found highly correlated with both LH plasma and progesterone intra-follicular concentrations might be the targets of LH-enhanced progesterone levels in the antral follicles.

Alternatively, testosterone exposure of fetal ovaries could have programmed theca cell differentiation and LH responsiveness on the long term. Indeed, most changes observed in ECM composition of the follicular theca in adulthood likely originate from the effects of androgen excess on theca cell precursors in the fetal ovary. The testosterone treatment, when administered to gestating ewes at a period encompassing ovarian development and follicle formation in female fetuses [16, 17], could affect the ovarian perifollicular stromal cells, known to express receptors to androgens and estrogens [20]. In mouse, the stromal cells of the fetal ovary appear to give rise to theca fibroblasts, perivascular smooth muscle cells, and interstitial ovarian tissue of postnatal ovaries [22, 76, 77]. From

our results, in the prenatally androgenized sheep ovaries, the COL7A1 immunostaining intensity was low in both the theca of small antral follicles and the interstitial stroma of ovarian cortex. This observation is consistent with the relationship existing between these tissues, although recent transcriptomic analyses have displayed some differences between interstitial stroma and theca interna in adult bovine ovaries [78]. Of interest, the expression of *FBN3*, encoding fibrillin 3, an ECM protein forming connective tissue microfibrils associated with elastin fibers, was also clearly decreased in the follicular theca of prenatally androgenized sheep. Fibrillin 3 is known to be highly expressed in the fetal bovine and human ovary, particularly in the perifollicular stroma of primordial and primary follicles, and can stimulate the collagen synthesis in fibroblasts by regulating TGFβ activity [79, 80]. Whether testosterone has sustainably affected the expression of fibrillin 3 in the stromal cells of fetal sheep ovaries, with long-term consequences on collagen expression in the theca cell lineage, remains to be established. In humans, *FBN3* has been found genetically associated with the risk of PCOS [81, 82].

In the ovaries of prenatally androgenized sheep, the changes in ECM composition of the follicular theca and the perifollicular stroma of follicles may have greatly weakened the stiffness of these tissues. Pioneering studies of Woodruff and Shea have shown that the rigidity of the extracellular matrix can impact follicle activation and growth [83, 84]. Mechanical factors contribute to primordial follicle activation through regulating signaling pathways including the Hippo pathway and the PI3K/AKT pathway [85, 86]. In humans, polycystic ovaries contain higher numbers of primary and secondary follicles, suggesting that abnormalities of follicle development in PCOS may have their root in the early stages of growth [87]. Of interest, the PCOS syndrome is associated with abnormal stiffness of ovarian cortex, and the dysregulated expression of some genes encoding extracellular matrix components has been reported in ovarian biopsies (containing a mixture of follicular and stromal components) recovered from both PCOS women and long-term androgen-treated female-to-male transsexuals [88]. Some differences exist between the lists of ECM genes dysregulated in PCOS women and in prenatally androgenized sheep, potentially explained by differences in species, ovarian tissue sampling and/or methodology of transcriptome analysis (microarray vs. RNA sequencing). However, both lists contain genes encoding factors strongly involved in tissue architecture, such as thrombospondin, collagen chains and disintegrin/metalloproteinases of the ADAMTS family.

From our results, we propose that exposure to testosterone excess can affect on the long term the local environment of follicles through effects on ECM composition, and activate intra-ovarian mechanisms stimulating the development of follicles up to the small antral stage. Similar actions of testosterone on the ECM composition and stiffness of non-ovarian urogenital tissues might also explain the predisposition of prenatally androgenized sheep to develop uterine cysts, pyometers and abnormal septa in the bladder. Whether *in utero* exposure to testosterone excess can also affect in adults the ECM composition of other organs such as the liver, pancreas, adipose tissue and skin, all known to be direct targets of testosterone [8, 89, 90], constitutes a new working hypothesis to decipher the mechanisms underlying the fetal programming by androgens and development of PCOS in adult life.

Ethical standards

All experimental procedures were approved by the French Agricultural and Scientific Research Government Committee (Approval number E37-175-2) and the Val de Loire ethics committee for animal experimentation

(Referral 2012-12-21, n°19), in accordance with the guidelines for Care and Use of Agricultural Animals in Agricultural Research and Teaching.

Competing interests

The authors declare that they have no conflict of interest.

Data availability

Raw Fastq files have been deposited in the NCBI sequenced Read archive under accession numbers SRR8776922-SRR8776937.

References

1. McAllister JM, Legro RS, Modi BP, Strauss JF, 3rd (2015) Functional genomics of PCOS: from GWAS to molecular mechanisms. Trends Endocrinol Metab 26:118-124. https://doi.org/10.1016/j.tem.2014.12.004
2. Dumesic DA, Richards JS (2013) Ontogeny of the ovary in polycystic ovary syndrome. Fertil Steril 100:23-38. https://doi.org/10.1016/j.fertnstert.2013.02.011
3. Tata B, Mimouni NEH, Barbotin AL, Malone SA, Loyens A, Pigny P, Dewailly D, Catteau-Jonard S, Sundstrom-Poromaa I, Piltonen TT, Dal Bello F, Medana C, Prevot V, Clasadonte J, Giacobini P (2018) Elevated prenatal anti-Mullerian hormone reprograms the fetus and induces polycystic ovary syndrome in adulthood. Nat Med 24:834-846. https://doi.org/10.1038/s41591-018-0035-5
4. Franks S, McCarthy MI, Hardy K (2006) Development of polycystic ovary syndrome: involvement of genetic and environmental factors. Int J Androl 29:278-285. https://doi.org/10.1111/j.1365-2605.2005.00623.x
5. Dumesic DA, Abbott DH, Padmanabhan V (2007) Polycystic ovary syndrome and its developmental origins. Rev Endocr Metab Disord 8:127-141. https://doi.org/10.1007/s11154-007-9046-0
6. Luque-Ramirez M, Escobar-Morreale HF (2016) Adrenal Hyperandrogenism and Polycystic Ovary Syndrome. Curr Pharm Des 22:5588-5602. https://doi.org/10.2174/1381612822666160720150625
7. Filippou P, Homburg R (2017) Is foetal hyperexposure to androgens a cause of PCOS? Hum Reprod Update 23:421-432. https://doi.org/10.1093/humupd/dmx013
8. Padmanabhan V, Veiga-Lopez A (2013) Sheep models of polycystic ovary syndrome phenotype. Mol Cell Endocrinol 373:8-20. https://doi.org/10.1016/j.mce.2012.10.005
9. Clarke IJ, Scaramuzzi RJ, Short RV (1977) Ovulation in prenatally androgenized ewes. J Endocrinol 73:385-389.
10. Birch RA, Padmanabhan V, Foster DL, Unsworth WP, Robinson JE (2003) Prenatal programming of reproductive neuroendocrine function: fetal androgen exposure produces progressive disruption of reproductive cycles in sheep. Endocrinology 144:1426-1434. https://doi.org/10.1210/en.2002-220965
11. Cardoso RC, Puttabyatappa M, Padmanabhan V (2015) Steroidogenic versus Metabolic Programming of Reproductive Neuroendocrine, Ovarian and Metabolic Dysfunctions. Neuroendocrinology 102:226-237. https://doi.org/10.1159/000381830
12. Steckler T, Wang J, Bartol FF, Roy SK, Padmanabhan V (2005) Fetal programming: prenatal testosterone treatment causes intrauterine growth retardation, reduces ovarian reserve and increases ovarian follicular recruitment. Endocrinology 146:3185-3193. https://doi.org/10.1210/en.2004-1444
13. Forsdike RA, Hardy K, Bull L, Stark J, Webber LJ, Stubbs S, Robinson JE, Franks S (2007) Disordered follicle development in ovaries of prenatally androgenized ewes. J Endocrinol 192:421-428. https://doi.org/10.1677/joe.1.07097
14. Smith P, Steckler TL, Veiga-Lopez A, Padmanabhan V (2009) Developmental programming: differential effects of prenatal testosterone and dihydrotestosterone on follicular recruitment, depletion of follicular reserve, and ovarian morphology in sheep. Biol Reprod 80:726-736. https://doi.org/10.1095/biolreprod.108.072801
15. Scaramuzzi RJ, Baird DT, Campbell BK, Driancourt MA, Dupont J, Fortune JE, Gilchrist RB, Martin GB, McNatty KP, McNeilly AS, Monget P, Monniaux D, Vinoles C, Webb R (2011) Regulation of folliculogenesis and the determination of ovulation rate in ruminants. Reprod Fertil Dev 23:444-467. https://doi.org/10.1071/RD09161

16. McNatty KP, Smith P, Hudson NL, Heath DA, Tisdall DJ, O WS, Braw-Tal R (1995) Development of the sheep ovary during fetal and early neonatal life and the effect of fecundity genes. J Reprod Fertil Supp. 49:123-135.
17. Juengel JL, Sawyer HR, Smith PR, Quirke LD, Heath DA, Lun S, Wakefield SJ, McNatty KP (2002) Origins of follicular cells and ontogeny of steroidogenesis in ovine fetal ovaries. Mol Cell Endocrinol 191:1-10. https://doi.org/10.1016/S0303-7207(02)00045-X
18. Veiga-Lopez A, Steckler TL, Abbott DH, Welch KB, MohanKumar PS, Phillips DJ, Refsal K, Padmanabhan V (2011) Developmental programming: impact of excess prenatal testosterone on intrauterine fetal endocrine milieu and growth in sheep. Biol Reprod 84:87-96. https://doi.org/10.1095/biolreprod.110.086686
19. Nieschlag E, Behre H (2010) Testosterone therapy. In: Nieschlag E, Behre HM, Nieschlag S (ed) Andrology: male reproductive health and dysfunction, 3rd edn. Springer, Berlin, Heidelberg, pp 437-456
20. Juengel JL, Heath DA, Quirke LD, McNatty KP (2006) Oestrogen receptor alpha and beta, androgen receptor and progesterone receptor mRNA and protein localisation within the developing ovary and in small growing follicles of sheep. Reproduction 131:81-92. https://doi.org/10.1530/rep.1.00704
21. Young JM, McNeilly AS (2010) Theca: the forgotten cell of the ovarian follicle. Reproduction 140:489-504. https://doi.org/10.1530/REP-10-0094
22. Richards JS, Ren YA, Candelaria N, Adams JE, Rajkovic A (2018) Ovarian Follicular Theca Cell Recruitment, Differentiation, and Impact on Fertility: 2017 Update. Endocr Rev 39:1-20. https://doi.org/10.1210/er.2017-00164
23. Hummitzsch K, Anderson RA, Wilhelm D, Wu J, Telfer EE, Russell DL, Robertson SA, Rodgers RJ (2015) Stem cells, progenitor cells, and lineage decisions in the ovary. Endocr Rev 36:65-91. https://doi.org/10.1210/er.2014-1079
24. Hogg K, McNeilly AS, Duncan WC (2011) Prenatal androgen exposure leads to alterations in gene and protein expression in the ovine fetal ovary. Endocrinology 152:2048-2059. https://doi.org/10.1210/en.2010-1219
25. Padmanabhan V, Salvetti NR, Matiller V, Ortega HH (2014) Developmental programming: prenatal steroid excess disrupts key members of intraovarian steroidogenic pathway in sheep. Endocrinology 155:3649-3660. https://doi.org/10.1210/en.2014-1266
26. Hogg K, Young JM, Oliver EM, Souza CJ, McNeilly AS, Duncan WC (2012) Enhanced thecal androgen production is prenatally programmed in an ovine model of polycystic ovary syndrome. Endocrinology 153:450-461. https://doi.org/10.1210/en.2011-1607
27. Manikkam M, Thompson RC, Herkimer C, Welch KB, Flak J, Karsch FJ, Padmanabhan V (2008) Developmental programming: impact of prenatal testosterone excess on pre- and postnatal gonadotropin regulation in sheep. Biol Reprod 78:648-660. https://doi.org/10.1095/biolreprod.107.063347
28. Robinson JE, Forsdike RA, Taylor JA (1999) In utero exposure of female lambs to testosterone reduces the sensitivity of the gonadotropin-releasing hormone neuronal network to inhibition by progesterone. Endocrinology 140:5797-5805. https://doi.org/10.1210/endo.140.12.7205
29. Guignot F, Baril G, Dupont F, Cognie Y, Folch J, Alabart JL, Poulin N, Beckers JF, Bed'hom B, Babilliot JM, Mermillod P (2009) Determination of sex and scrapie resistance genotype in preimplantation ovine embryos. Mol Reprod Dev 76:183-190. https://doi.org/10.1002/mrd.20940
30. Estienne A, Pierre A, di Clemente N, Picard JY, Jarrier P, Mansanet C, Monniaux D, Fabre S (2015) Anti-Mullerian hormone regulation by the bone morphogenetic proteins in the sheep ovary: deciphering a direct regulatory pathway. Endocrinology 156:301-313. https://doi.org/10.1210/en.2014-1551
31. Hochereau-de Reviers MT, Perreau C, Pisselet C, Fontaine I, Monet-Kuntz C (1990) Comparisons of endocrinological and testis parameters in 18-month-old Ile de France and Romanov rams. Dom Anim Endocr 7:63-73.
32. Canepa S, Lainé AL, Bluteau A, Fagu C, Flon C, Monniaux D (2008) Validation d'une méthode immunoenzymatique pour le dosage de la progestérone dans le plasma des ovins et des bovins. Cahier des Techniques de l'Inra 64:19-30.
33. Cadoret V, Frapsauce C, Jarrier P, Maillard V, Bonnet A, Locatelli Y, Royere D, Monniaux D, Guerif F, Monget P (2017) Molecular evidence that follicle development is accelerated in vitro compared to in vivo. Reproduction 153:493-508. https://doi.org/10.1530/REP-16-0627
34. Faure MO, Nicol L, Fabre S, Fontaine J, Mohoric N, McNeilly A, Taragnat C (2005) BMP-4 inhibits follicle-stimulating hormone secretion in ewe pituitary. J Endocrinol 186:109-121. https://doi.org/10.1677/joe.1.05988
35. Talebi R, Ahmadi A, Afraz F, Sarry J, Plisson-Petit F, Genet C, Fabre S (2018) Transcriptome analysis of ovine granulosa cells reveals differences between small antral follicles collected during the follicular and luteal phases. Theriogenology 108:103-117. https://doi.org/10.1016/j.theriogenology.2017.11.027

36. Varet H, Brillet-Gueguen L, Coppee JY, Dillies MA (2016) SARTools: A DESeq2- and EdgeR-Based R Pipeline for Comprehensive Differential Analysis of RNA-Seq Data. PLoS One 11:e0157022. https://doi.org/10.1371/journal.pone.0157022
37. Love MI, Huber W, Anders S (2014) Moderated estimation of fold change and dispersion for RNA-seq data with DESeq2. Genome Biol 15:550. https://doi.org/10.1186/s13059-014-0550-8
38. Benjamini Y, Hochberg Y (1995) Controlling the False Discovery Rate: A Practical and Powerful Approach to Multiple Testing. J Roy Stat Soc Series B (Methodological) 57:289-300.
39. Smedley D, Haider S, Durinck S et al (2015) The BioMart community portal: an innovative alternative to large, centralized data repositories. Nucleic Acids Res 43:W589-598. https://doi.org/10.1093/nar/gkv350
40. Louis A, Nguyen NT, Muffato M, Roest Crollius H (2015) Genomicus update 2015: KaryoView and MatrixView provide a genome-wide perspective to multispecies comparative genomics. Nucleic Acids Res 43:D682-689. https://doi.org/10.1093/nar/gku1112
41. Chen EY, Tan CM, Kou Y, Duan Q, Wang Z, Meirelles GV, Clark NR, Ma'ayan A (2013) Enrichr: interactive and collaborative HTML5 gene list enrichment analysis tool. BMC Bioinformatics 14:128. https://doi.org/10.1186/1471-2105-14-128
42. Kuleshov MV, Jones MR, Rouillard AD, Fernandez NF, Duan Q, Wang Z, Koplev S, Jenkins SL, Jagodnik KM, Lachmann A, McDermott MG, Monteiro CD, Gundersen GW, Ma'ayan A (2016) Enrichr: a comprehensive gene set enrichment analysis web server 2016 update. Nucleic Acids Res 44:W90-97. https://doi.org/10.1093/nar/gkw377
43. Le Cao KA, Rossouw D, Robert-Granie C, Besse P (2008) A sparse PLS for variable selection when integrating omics data. Stat Appl Genet Mol Biol 7:Article 35. https://doi.org/10.2202/1544-6115.1390
44. Rohart F, Gautier B, Singh A, Le Cao KA (2017) mixOmics: An R package for 'omics feature selection and multiple data integration. PLoS Comput Biol 13:e1005752. https://doi.org/10.1371/journal.pcbi.1005752
45. Livak KJ, Schmittgen TD (2001) Analysis of relative gene expression data using real-time quantitative PCR and the 2(-Delta Delta C(T)) Method. Methods 25:402-408. https://doi.org/10.1006/meth.2001.1262
46. Pfaffl MW, Tichopad A, Prgomet C, Neuvians TP (2004) Determination of stable housekeeping genes, differentially regulated target genes and sample integrity: BestKeeper--Excel-based tool using pair-wise correlations. Biotechnol Lett 26:509-515.
47. Drouilhet L, Mansanet C, Sarry J, Tabet K, Bardou P, Woloszyn F, Lluch J, Harichaux G, Viguie C, Monniaux D, Bodin L, Mulsant P, Fabre S (2013) The highly prolific phenotype of Lacaune sheep is associated with an ectopic expression of the B4GALNT2 gene within the ovary. PLoS Genet 9:e1003809. https://doi.org/10.1371/journal.pgen.1003809
48. Shumway RH, Stoffer DS (2011) Time series analysis and its applications with R examples. Springer, New York, Dordrecht, Heidelberg, London
49. Torres-Rovira L, Gonzalez-Bulnes A, Succu S, Spezzigu A, Manca ME, Leoni GG, Sanna M, Pirino S, Gallus M, Naitana S, Berlinguer F (2014) Predictive value of antral follicle count and anti-Mullerian hormone for follicle and oocyte developmental competence during the early prepubertal period in a sheep model. Reprod Fertil Dev 26:1094-1106. https://doi.org/10.1071/RD13190
50. Torres-Rovira L, Succu S, Pasciu V, Manca ME, Gonzalez-Bulnes A, Leoni GG, Pennino MG, Spezzigu A, Gallus M, Dattena M, Monniaux D, Naitana S, Berlinguer F (2016) Postnatal pituitary and follicular activation: a revisited hypothesis in a sheep model. Reproduction 151:215-225. https://doi.org/10.1530/REP-15-0316
51. Campbell BK, Clinton M, Webb R (2012) The role of anti-Mullerian hormone (AMH) during follicle development in a monovulatory species (sheep). Endocrinology 153:4533-4543. https://doi.org/10.1210/en.2012-1158
52. Cheon KY, Chung YJ, Cho HH, Kim MR, Cha JH, Kang CS, Lee JY, Kim JH (2018) Expression of Mullerian-Inhibiting Substance/Anti-Mullerian Hormone Type II Receptor in the Human Theca Cells. J Clin Endocrinol Metab 103:3376-3385. https://doi.org/10.1210/jc.2018-00549
53. Monniaux D, Cadoret V, Clément F, Dalbies-Tran R, Elis S, Fabre S, Maillard V, Monget P, Uzbekova S (2019) Folliculogenesis. In: I Huhtaniemi, L Martini (ed) Encyclopedia of Endocrine Diseases, 2nd edn. Elsevier, Oxford, pp 377-398
54. Knight PG, Glister C (2006) TGF-beta superfamily members and ovarian follicle development. Reproduction 132:191-206. https://doi.org/10.1530/rep.1.01074
55. Lamm CG, Hastie PM, Evans NP, Robinson JE (2012) Masculinization of the distal tubular and external genitalia in female sheep with prenatal androgen exposure. Vet Pathol 49:546-551. https://doi.org/10.1177/0300985811419533
56. Padmanabhan V, Veiga-Lopez A, Abbott DH, Recabarren SE, Herkimer C (2010) Developmental programming: impact of prenatal testosterone excess and postnatal weight gain on insulin sensitivity

index and transfer of traits to offspring of overweight females. Endocrinology 151:595-605. https://doi.org/10.1210/en.2009-1015

57. Nada SE, Thompson RC, Padmanabhan V (2010) Developmental programming: differential effects of prenatal testosterone excess on insulin target tissues. Endocrinology 151:5165-5173. https://doi.org/10.1210/en.2010-0666
58. Hogg K, Wood C, McNeilly AS, Duncan WC (2011) The in utero programming effect of increased maternal androgens and a direct fetal intervention on liver and metabolic function in adult sheep. PLoS One 6:e24877. https://doi.org/10.1371/journal.pone.0024877
59. Cardoso RC, Veiga-Lopez A, Moeller J, Beckett E, Pease A, Keller E, Madrigal V, Chazenbalk G, Dumesic D, Padmanabhan V (2016) Developmental Programming: Impact of Gestational Steroid and Metabolic Milieus on Adiposity and Insulin Sensitivity in Prenatal Testosterone-Treated Female Sheep. Endocrinology 157:522-535. https://doi.org/10.1210/en.2015-1565
60. Dupont J, Scaramuzzi RJ (2016) Insulin signalling and glucose transport in the ovary and ovarian function during the ovarian cycle. Biochem J 473:1483-1501. https://doi.org/10.1042/BCJ20160124
61. Visser JA, de Jong FH, Laven JS, Themmen AP (2006) Anti-Mullerian hormone: a new marker for ovarian function. Reproduction 131:1-9. https://doi.org/10.1530/rep.1.00529
62. Anderson RA (2012) What does anti-Mullerian hormone tell you about ovarian function? Clin Endocrinol (Oxf) 77:652-655. https://doi.org/10.1111/j.1365-2265.2012.04451.x
63. Monniaux D, Drouilhet L, Rico C, Estienne A, Jarrier P, Touzé JL, Sapa J, Phocas F, Dupont J, Dalbies-Tran R, Fabre S (2013) Regulation of anti-Mullerian hormone production in domestic animals. Reprod Fertil Dev 25:1-16. https://doi.org/10.1071/RD12270
64. Monniaux D, Caraty A, Clément F, Dalbies-Tran R, Dupont J, Fabre S, Gérard N, Mermillod P, Monget P, Uzbekova S (2009) Développement folliculaire ovarien et ovulation chez les mammifères. INRA Prod Anim 22:59-76.
65. Rawlings NC, Evans AC, Honaramooz A, Bartlewski PM (2003) Antral follicle growth and endocrine changes in prepubertal cattle, sheep and goats. Anim Reprod Sci 78:259-270.
66. Padmanabhan V, Manikkam M, Recabarren S, Foster D (2006) Prenatal testosterone excess programs reproductive and metabolic dysfunction in the female. Mol Cell Endocrinol 246:165-174. https://doi.org/10.1016/j.mce.2005.11.016
67. Marinkovich MP (2007) Tumour microenvironment: laminin 332 in squamous-cell carcinoma. Nat Rev Cancer 7:370-380. https://doi.org/10.1038/nrc2089
68. Cianfarani F, Zambruno G, Castiglia D, Odorisio T (2017) Pathomechanisms of Altered Wound Healing in Recessive Dystrophic Epidermolysis Bullosa. Am J Pathol 187:1445-1453. https://doi.org/10.1016/j.ajpath.2017.03.003
69. Rattenholl A, Pappano WN, Koch M, Keene DR, Kadler KE, Sasaki T, Timpl R, Burgeson RE, Greenspan DS, Bruckner-Tuderman L (2002) Proteinases of the bone morphogenetic protein-1 family convert procollagen VII to mature anchoring fibril collagen. J Biol Chem 277:26372-26378. https://doi.org/10.1074/jbc.M203247200
70. Faletra F, D'Adamo AP, Bruno I, Athanasakis E, Biskup S, Esposito L, Gasparini P (2014) Autosomal recessive Stickler syndrome due to a loss of function mutation in the COL9A3 gene. Am J Med Genet A 164A:42-47. https://doi.org/10.1002/ajmg.a.36165
71. Lamande SR, Bateman JF (2018) Collagen VI disorders: Insights on form and function in the extracellular matrix and beyond. Matrix Biol. 71-72:348-367. https://doi.org/10.1016/j.matbio.2017.12.008
72. Hatzirodos N, Hummitzsch K, Irving-Rodgers HF, Rodgers RJ (2014) Transcriptome profiling of the theca interna in transition from small to large antral ovarian follicles. PLoS One 9:e97489. https://doi.org/10.1371/journal.pone.0097489
73. Hatzirodos N, Irving-Rodgers HF, Hummitzsch K, Rodgers RJ (2014) Transcriptome profiling of the theca interna from bovine ovarian follicles during atresia. PLoS One 9:e99706. https://doi.org/10.1371/journal.pone.0099706
74. Sarma HN, Manikkam M, Herkimer C, Dell'Orco J, Welch KB, Foster DL, Padmanabhan V (2005) Fetal programming: excess prenatal testosterone reduces postnatal luteinizing hormone, but not follicle-stimulating hormone responsiveness, to estradiol negative feedback in the female. Endocrinology 146:4281-4291. https://doi.org/10.1210/en.2005-0322
75. Christenson LK, Gunewardena S, Hong X, Spitschak M, Baufeld A, Vanselow J (2013) Research resource: preovulatory LH surge effects on follicular theca and granulosa transcriptomes. Mol Endocrinol 27:1153-1171. https://doi.org/10.1210/me.2013-1093
76. Liu C, Peng J, Matzuk MM, Yao HH (2015) Lineage specification of ovarian theca cells requires multicellular interactions via oocyte and granulosa cells. Nat Commun 6:6934. https://doi.org/10.1038/ncomms7934

77. Rotgers E, Jorgensen A, Yao HH (2018) At the Crossroads of Fate-Somatic Cell Lineage Specification in the Fetal Gonad. Endocr Rev 39:739-759. https://doi.org/10.1210/er.2018-00010
78. Hummitzsch K, Hatzirodos N, Macpherson A, Schwartz J, Rodgers RJ, Irving-Rodgers HF (2019) Transcriptome analyses of ovarian stroma; tunica albuginea, interstitium and theca interna. Reproduction. https://doi.org/10.1530/REP-18-0323
79. Jordan CD, Bohling SD, Charbonneau NL, Sakai LY (2010) Fibrillins in adult human ovary and polycystic ovary syndrome: is fibrillin-3 affected in PCOS? J Histochem Cytochem 58:903-915. https://doi.org/10.1369/jhc.2010.956615
80. Hatzirodos N, Bayne RA, Irving-Rodgers HF, Hummitzsch K, Sabatier L, Lee S, Bonner W, Gibson MA, Rainey WE, Carr BR, Mason HD, Reinhardt DP, Anderson RA, Rodgers RJ (2011) Linkage of regulators of TGF-beta activity in the fetal ovary to polycystic ovary syndrome. FASEB J 25:2256-2265. https://doi.org/10.1096/fj.11-181099
81. Urbanek M, Sam S, Legro RS, Dunaif A (2007) Identification of a polycystic ovary syndrome susceptibility variant in fibrillin-3 and association with a metabolic phenotype. J Clin Endocrinol Metab 92:4191-4198. https://doi.org/10.1210/jc.2007-0761
82. Ewens KG, Stewart DR, Ankener W, Urbanek M, McAllister JM, Chen C, Baig KM, Parker SC, Margulies EH, Legro RS, Dunaif A, Strauss JF, 3rd, Spielman RS (2010) Family-based analysis of candidate genes for polycystic ovary syndrome. J Clin Endocrinol Metab. 95:2306-2315. https://doi.org/10.1210/jc.2009-2703
83. West ER, Shea LD, Woodruff TK (2007) Engineering the follicle microenvironment. Semin Reprod Med 25:287-299. https://doi.org/10.1055/s-2007-980222
84. Woodruff TK, Shea LD (2011) A new hypothesis regarding ovarian follicle development: ovarian rigidity as a regulator of selection and health. J Assist Reprod Genet 28:3-6. https://doi.org/10.1007/s10815-010-9478-4
85. Cheng Y, Feng Y, Jansson L, Sato Y, Deguchi M, Kawamura K, Hsueh AJ (2015) Actin polymerization-enhancing drugs promote ovarian follicle growth mediated by the Hippo signaling effector YAP. FASEB J 29:2423-30. https://doi.org/10.1096/fj.14-267856
86. Hsueh AJ, Kawamura K, Cheng Y, Fauser BC (2015) Intraovarian control of early folliculogenesis. Endocr Rev 36:1-24. https://doi.org/10.1210/er.2014-1020
87. Franks S, Stark J, Hardy K (2008) Follicle dynamics and anovulation in polycystic ovary syndrome. Hum Reprod Update 14:367-78. https://doi.org/10.1093/humupd/dmn015
88. Jansen E, Laven JS, Dommerholt HB, Polman J, van Rijt C, van den Hurk C, Westland J, Mosselman S, Fauser BC (2004) Abnormal gene expression profiles in human ovaries from polycystic ovary syndrome patients. Mol Endocrinol 18:3050-63. https://doi.org/10.1210/me.2004-0074
89. Puttabyatappa M, Lu C, Martin JD, Chazenbalk G, Dumesic D, Padmanabhan V (2018) Developmental Programming: Impact of Prenatal Testosterone Excess on Steroidal Machinery and Cell Differentiation Markers in Visceral Adipocytes of Female Sheep. Reprod Sci 25:1010-1023. https://doi.org/10.1177/1933719117746767
90. Tonellotto Dos Santos J, Escariao da Nobrega J, Jr., Serrano Mujica LK, Dos Santos Amaral C, Machado FA, Manta MW, Rizzetti TM, Zanella R, Fighera R, Antoniazzi AQ, Goncalves PBD, Comim FV (2018) Prenatal Androgenization of Ewes as a Model of Hirsutism in Polycystic Ovary Syndrome. Endocrinology 159:4056-4064. https://doi.org/10.1210/en.2018-00781

Figure Captions

Fig. 1 Abdominal and ovarian magnetic resonance (MR) images of 8-weeks old lambs. Panel a illustrates a MR abdominal image (axial slice) showing both ovaries. LO: left ovary, RO: right ovary, dm: dorsal muscles, r: rumen, fn: femoral neck, g: gut. Panel b depicts MR ovarian images from different lambs, with antral follicles appearing as white ovoid structures. The numbers and sizes of ovarian follicles were highly variable between lambs in both the Control (group C) and the Testosterone-treated (group T) groups

Fig. 2 Populations of antral follicles equal to and larger than 1 mm in diameter, analyzed at 8, 18, 26 and 52 weeks of age by MRI. The figure shows the results of follicle counting on both ovaries of 8 animals in each experimental group. Follicles were allocated to 3 size classes: 1–3 mm (including 1 and 3 mm diameter follicles), 3–5 mm (including 5 mm diameter follicles) and > 5 mm in diameter. At each age of animals and for each size class of follicles, the comparison of follicle numbers between groups was done using t test, with Welch's correction when variances were heterogeneous. For [1-3] mm follicles, *: $p < 0.05$, ***: $p < 0.001$, group T vs. group C

Fig. 3 Plasma concentrations of ovarian hormones from birth to 67 weeks of age. Data represent AMH (panels a and b) and testosterone (panels c and d) concentrations in plasma samples recovered every 2 weeks from birth to 26 weeks of age, then monthly afterwards, on 8 animals in each experimental group. The hormonal profiles are depicted in panels a and c, and the average hormonal concentrations during 4 different periods of postnatal life in panels b and d. For each panel, the comparison of hormonal concentrations between groups was done using Mann-Whitney test. (*): $p < 0.1$, *: $p < 0.05$, group T vs. group C

Fig. 4 Plasma concentrations of pituitary hormones from birth to 67 weeks of age. Data represent FSH (panels a and b) and LH (panels c and d) concentrations in plasma samples recovered every 2 weeks from birth to 26 weeks of age, then monthly afterwards, on 8 animals in each experimental group. The hormonal profiles are depicted in panels a and c, and the average hormonal concentrations during 4 different periods of postnatal life, in panels b and d. For each panel, the comparison of hormonal concentrations between groups was done using Mann-Whitney test. (*): $p < 0.1$, *: $p < 0.05$, **: $p < 0.01$, group T vs. group C

Fig. 5 Populations of antral follicles and hormonal concentrations in follicular fluids at 67 weeks of age. After animal slaughtering (group C: n=9; group T: n=7), both ovaries were dissected to recover follicles at least 1 mm in diameter. Follicles were allocated to 3 size classes: 1–3 mm (including 1 and 3 mm diameter follicles), 3–5 mm (including 5 mm diameter follicles) and > 5 mm in diameter, and follicular fluids were collected. The figure shows the numbers of follicles per animal (panel a) and the intra-follicular concentrations of AMH (panel b), testosterone (panel c), estradiol (panel d) and progesterone (panel e). For each panel, the means were compared between groups using t test, with Welch's correction when variances were heterogeneous. (*): $p < 0.1$, *: $p < 0.05$, **: $p < 0.01$, group T vs. group C. Within each group, intra-follicular hormonal concentrations between the different size classes of follicles were compared using Kruskal-Wallis test. In each panel, different letters indicate significant differences ($p < 0.05$) between follicular classes within each group

Fig. 6 Gene network linked with collagen signaling pathways. The network was obtained through pathway analysis *via* Ingenuity Pathway Analysis software (netw8_COL7A1, QIAGEN). In this network, 29 genes exhibit a lower (green) or higher (red) expression in the follicular theca of 1-3 mm diameter follicles from animals of group T, compared to group C. The top functions corresponding to this network include "Cancer", "Connective Tissue Disorders", "Organismal Injury and Abnormalities"

Fig. 7 Immunostaining of COL7A1 and SMOC2 in the cortex and small antral follicles of ovaries at 67 weeks of age. For the detection of each protein, immunohistochemistry experiments were performed simultaneously on ovarian sections from both experimental groups. For COL7A1, the cortex and the theca of small ovarian follicles exhibited a lower staining in the ovaries of group T, compared to group C (panels a-f). For SMOC2, the theca of small ovarian follicles exhibited a higher staining in the ovaries of group T, compared to group C, but cortex staining was similar between groups (panels g-l). Primordial follicles are indicated by arrowheads. Oe: ovarian epithelium, C: cortex, T: theca, G: granulosa, O: oocyte, A: antrum. Bar = 100 µm

Fig. 8 Network of positive and negative covariances between differentially expressed genes and hormonal measures. Blue nodes: hormonal variables, black nodes: gene variables. Only annotated genes were reported in this network. Green and red lines = respectively negative and positive correlations, ranging from 0.7 to 0.86 in absolute value

Table 1 Top five ontologies and pathways through the enrichment analysis tool Enrichr

Gene Ontology Term 2018*	GO Term ID	Overlap	Adj. P-value	Z-score	Combined Score
Molecular Function					
Transforming growth factor beta (TGFB) binding	GO:0050431	6/20	7.41E-03	-2.23	23.65
Metal ion binding	GO:0046872	31/443	7.41E-03	-1.14	11.96
Insulin-like growth factor I binding	GO:0031994	5/14	8.03E-03	-2.09	20.90
Type 1 TGFB receptor binding	GO:0034713	4/9	1.08E-03	-2.84	26.00
Microtubule binding	GO:0008017	17/196	1.32E-02	-1.06	9.33
Cellular Component					
Endoplasmic reticulum lumen	GO:0005788	28/271	7.33E-06	-1.55	26.60
Focal adhesion	GO:0005925	28/357	9.42E-04	-1.12	13.06
Lysosomal lumen	GO:0043202	10/87	2.71E-03	-1.71	13.41
Pathway Term 2016*	**GO Term ID**	**Overlap**	**Adj. P-value**	**Z-score**	**Combined Score**
KEGG					
Extracellular matrix -receptor interaction	hsa04512	11/82	1.19E-03	-1.71	17.00
Wiki Pathways					
XPodNet - protein-protein interactions in the podocyte expanded by STRING	WP2309	53/808	1.03E-04	-2.23	33.21
PodNet: protein-protein interactions in the podocyte	WP2310	26/305	6.50E-04	-2.14	26.41
Reactome					
Extracellular matrix organization	HSA-1474244	33/283	7.83E-08	-2.11	48.82
Collagen biosynthesis and modifying enzymes	HSA-1650814	14/63	2.21E-06	-2.01	37.81
Collagen formation	HSA-1474290	16/85	2.21E-06	-2.01	37.57
Integrin cell surface interactions	HSA-216083	13/67	2.91E-05	-1.97	31.26
Syndecan interactions	HSA-3000170	6/20	4.30E-04	-1.88	19.99

* Only terms with an adjusted P-value < 0.05 were selected in each term category

Table 2 Differential expression in theca cells of twelve genes involved in extracellular matrix organization or intercellular junctions, from the results of RNA sequencing and RT-qPCR analyses

	RNAseq*		RT-qPCR$	
Gene Symbol	**FC**	**adj. p-value**	**FC**	**p-value**
SMOC2	1.53	1.8E-02	2.04	2.03E-02
SMOC1	1.89	5.5E-06	1.51	4.71E-02
HS6ST2	1.87	7.0E-10	2.07	1.77E-02
TLL2	1.64	4.4E-04	1.87	1.86E-03
DSP	1.65	6.1E-06	1.64	1.35E-01(*n.s.*)
CDH2	1.60	1.1E-04	1.20	4.07E-01(*n.s.*)
ITGA6	1.54	2.9E-07	1.61	4.92E-03
EMILIN2	0.63	1.0E-02	0.29	1.33E-04
COL9A3	0.67	2.9E-02	0.61	1.01E-02
SERPINF1	0.62	5.9E-03	0.84	7.34E-01(*n.s.*)
FBN3	0.40	7.3E-15	0.24	2.65E-07
COL7A1	0.41	9.0E-10	0.32	4.34E-03

*The fold changes (FC) of expression ratio group T/group C and the adjusted p-values were obtained by RNA sequencing followed by DESEQ2 analysis, on 4 samples from each experimental group of lambs. $The fold changes (FC) of expression ratio group T/group C and the p-values were obtained by RT-qPCR followed by t test, on 17 samples from each experimental group of lambs. *(n.s.)* = not significant

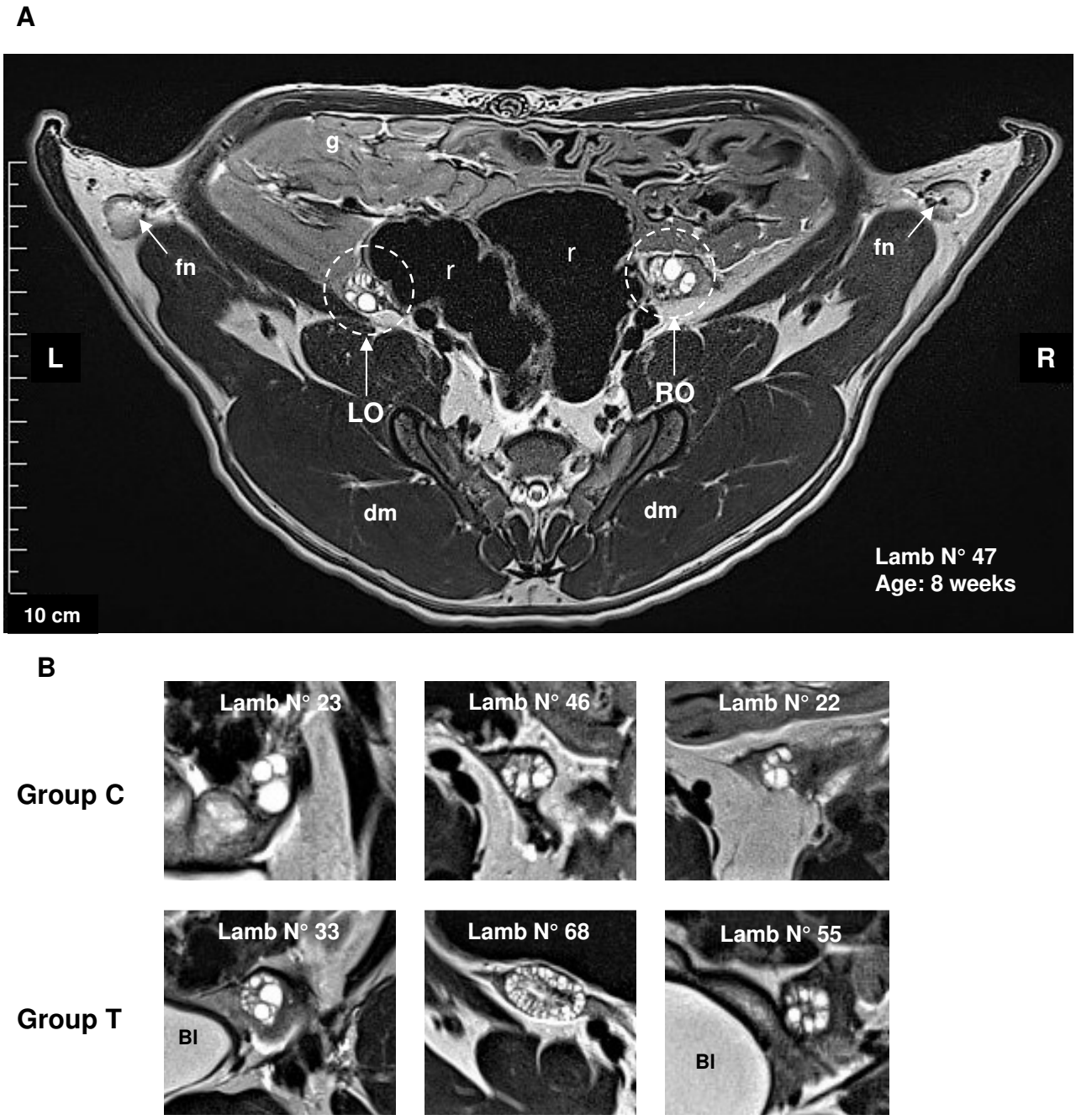
A
g
fn
r
r
fn
L
R
LO
RO
dm
dm
Lamb N° 47
Age: 8 weeks
10 cm
B
Group C
Lamb N° 23
Lamb N° 46
Lamb N° 22
Group T
Lamb N° 33
Bl
Lamb N° 68
Lamb N° 55
Bl

Figure 1

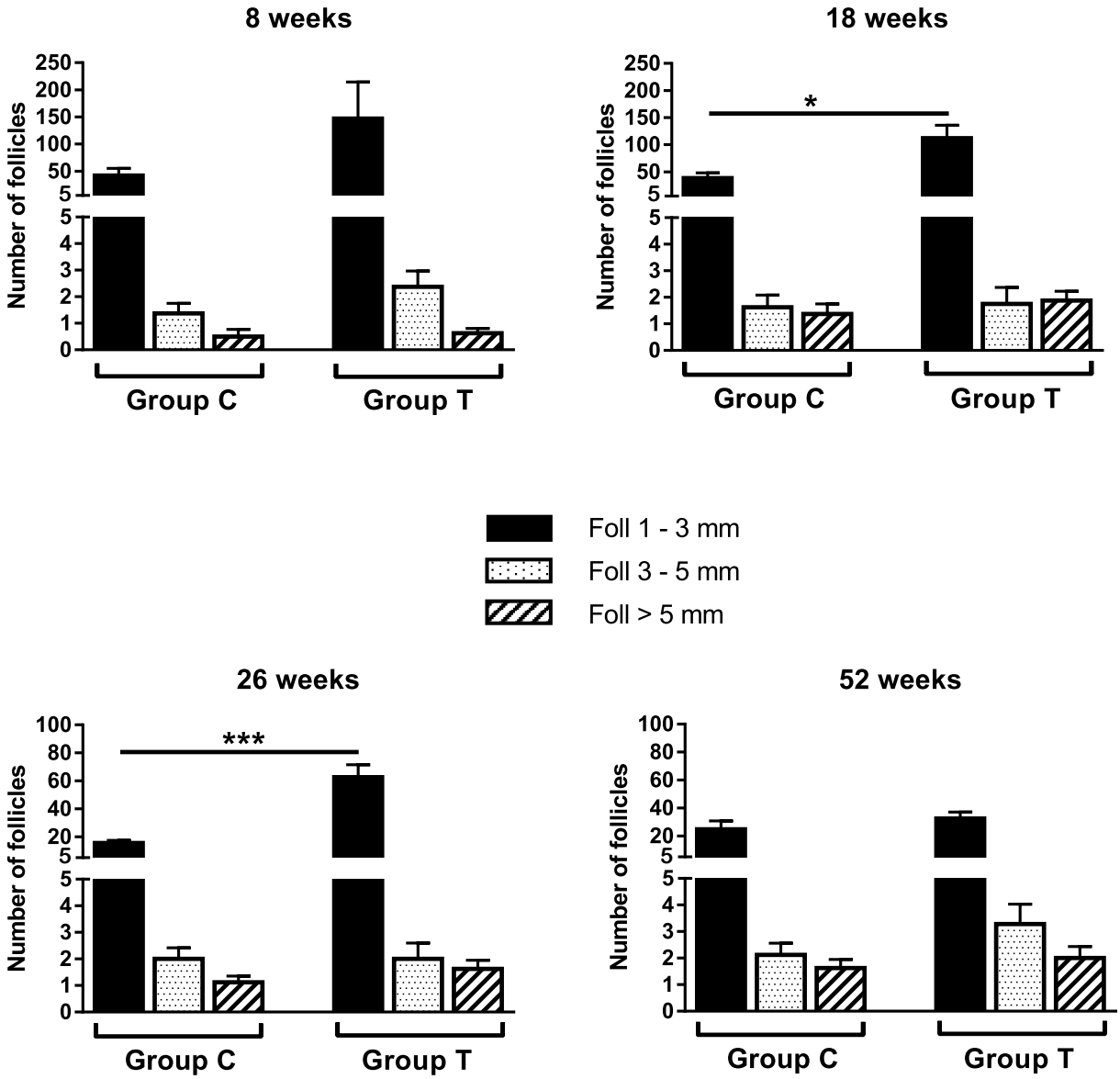
8 weeks
18 weeks
Number of follicles
250
200
150
100
50
5
4
3
2
1
0
*
Group C
Group T
Foll 1 - 3 mm
Foll 3 - 5 mm
Foll > 5 mm
26 weeks
52 weeks
100
80
60
40
20
***

Figure 2

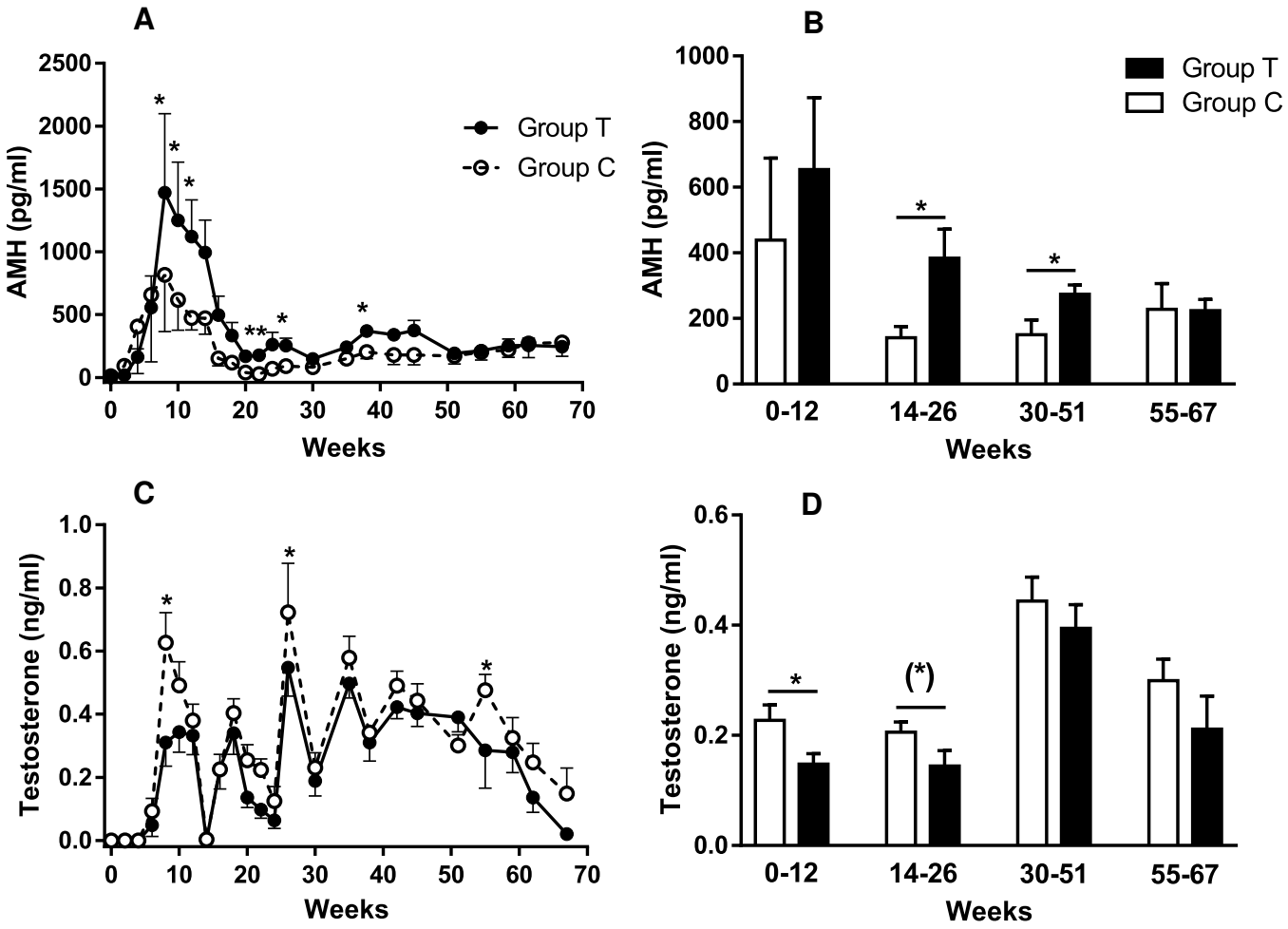
A
AMH (pg/ml)
2500
2000
1500
1000
500
0
Group T
Group C
0
10
20
30
40
50
60
70
Weeks
B
AMH (pg/ml)
1000
800
600
400
200
0
Group T
Group C
0-12
14-26
30-51
55-67
Weeks
C
Testosterone (ng/ml)
1.0
0.8
0.6
0.4
0.2
0.0
0
10
20
30
40
50
60
70
Weeks
D
Testosterone (ng/ml)
0.6
0.4
0.2
0.0
(*)
0-12
14-26
30-51
55-67
Weeks

Figure 3

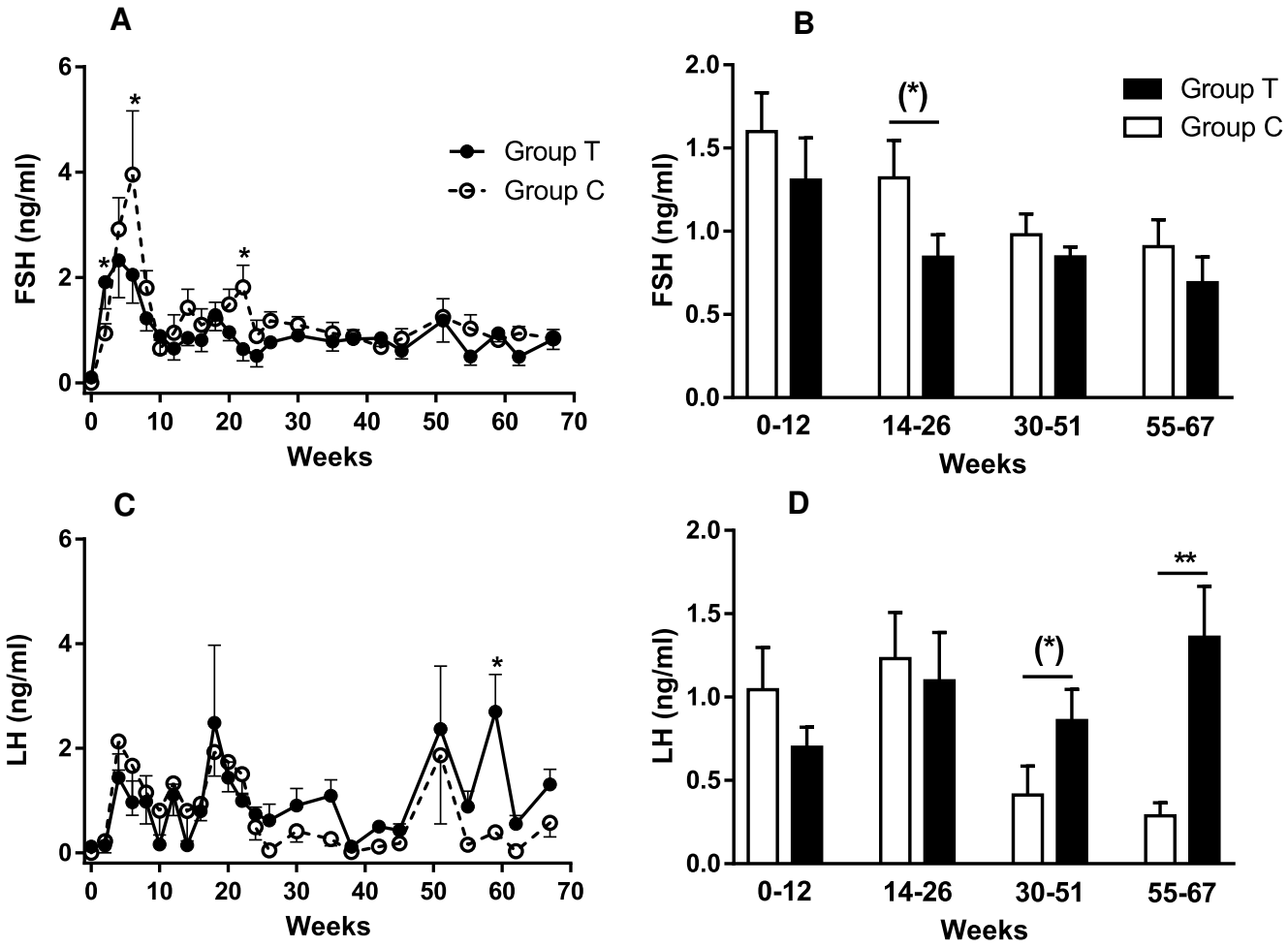
A
FSH (ng/ml)
Weeks
Group T
Group C
B
FSH (ng/ml)
(*)
0-12
14-26
30-51
55-67
Weeks
Group T
Group C
C
LH (ng/ml)
Weeks
D
LH (ng/ml)
(*)
**
0-12
14-26
30-51
55-67
Weeks

Figure 4

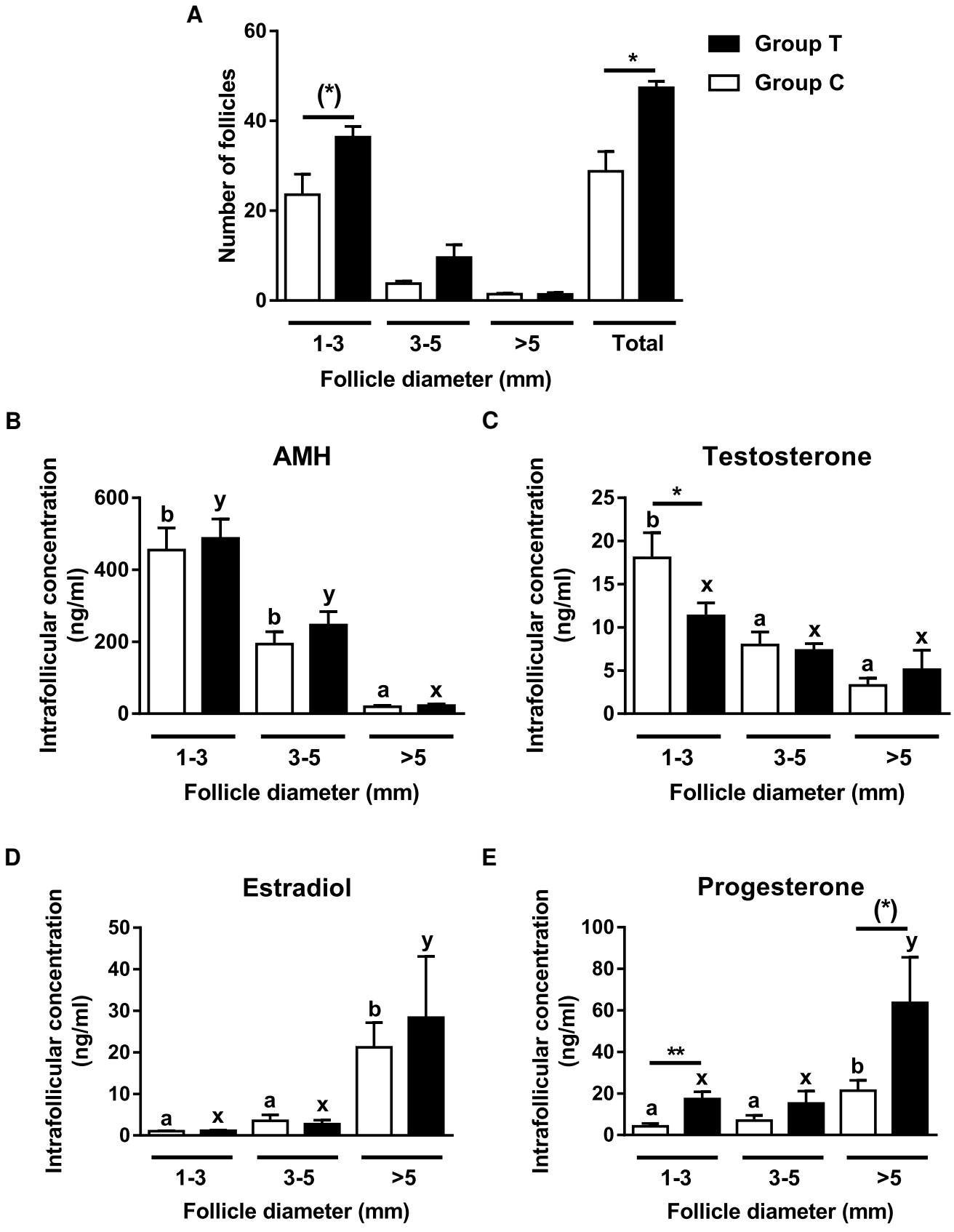
A
Number of follicles
60
40
20
0
(*)
*
Group T
Group C
1-3
3-5
>5
Total
Follicle diameter (mm)
B
AMH
Intrafollicular concentration (ng/ml)
600
400
200
0
b
y
b
y
a
x
1-3
3-5
>5
Follicle diameter (mm)
C
Testosterone
Intrafollicular concentration (ng/ml)
25
20
15
10
5
0
*
b
x
a
x
a
x
1-3
3-5
>5
Follicle diameter (mm)
D
Estradiol
Intrafollicular concentration (ng/ml)
50
40
30
20
10
0
a
x
a
x
b
y
1-3
3-5
>5
Follicle diameter (mm)
E
Progesterone
Intrafollicular concentration (ng/ml)
100
80
60
40
20
0
**
(*)
a
x
a
x
b
y
1-3
3-5
>5
Follicle diameter (mm)

Figure 5

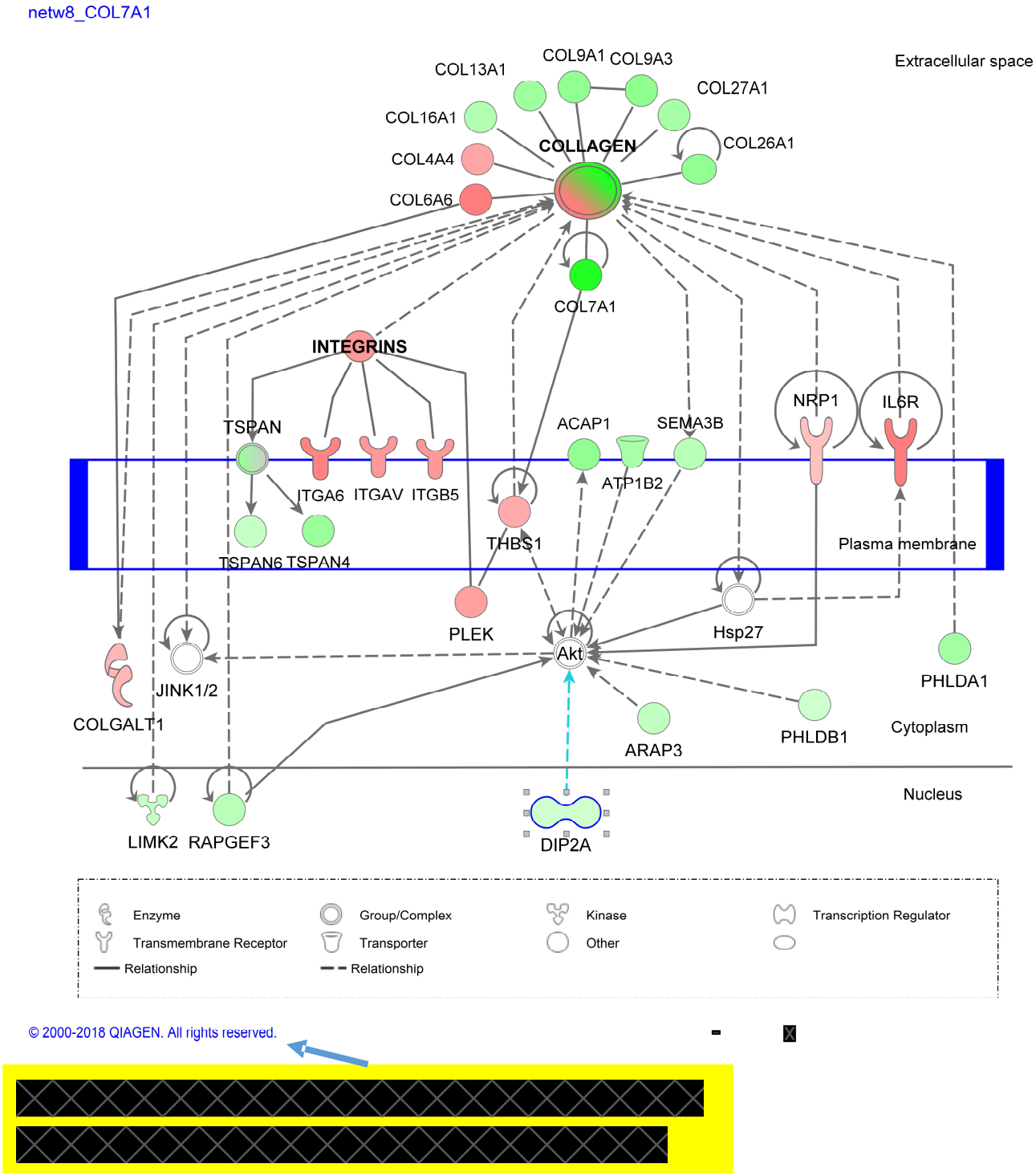
netw8_COL7A1
Extracellular space
COL13A1
COL9A1
COL9A3
COL27A1
COL16A1
COLLAGEN
COL26A1
COL4A4
COL6A6
COL7A1
INTEGRINS
TSPAN
ITGA6
ITGAV
ITGB5
ACAP1
SEMA3B
NRP1
IL6R
ATP1B2
TSPAN6
TSPAN4
THBS1
Plasma membrane
PLEK
Hsp27
Akt
PHLDA1
JINK1/2
COLGALT1
PHLDB1
Cytoplasm
ARAP3
Nucleus
LIMK2
RAPGEF3
DIP2A
Enzyme
Group/Complex
Kinase
Transcription Regulator
Transmembrane Receptor
Transporter
Other
Relationship
Relationship
© 2000-2018 QIAGEN. All rights reserved.

Figure 6

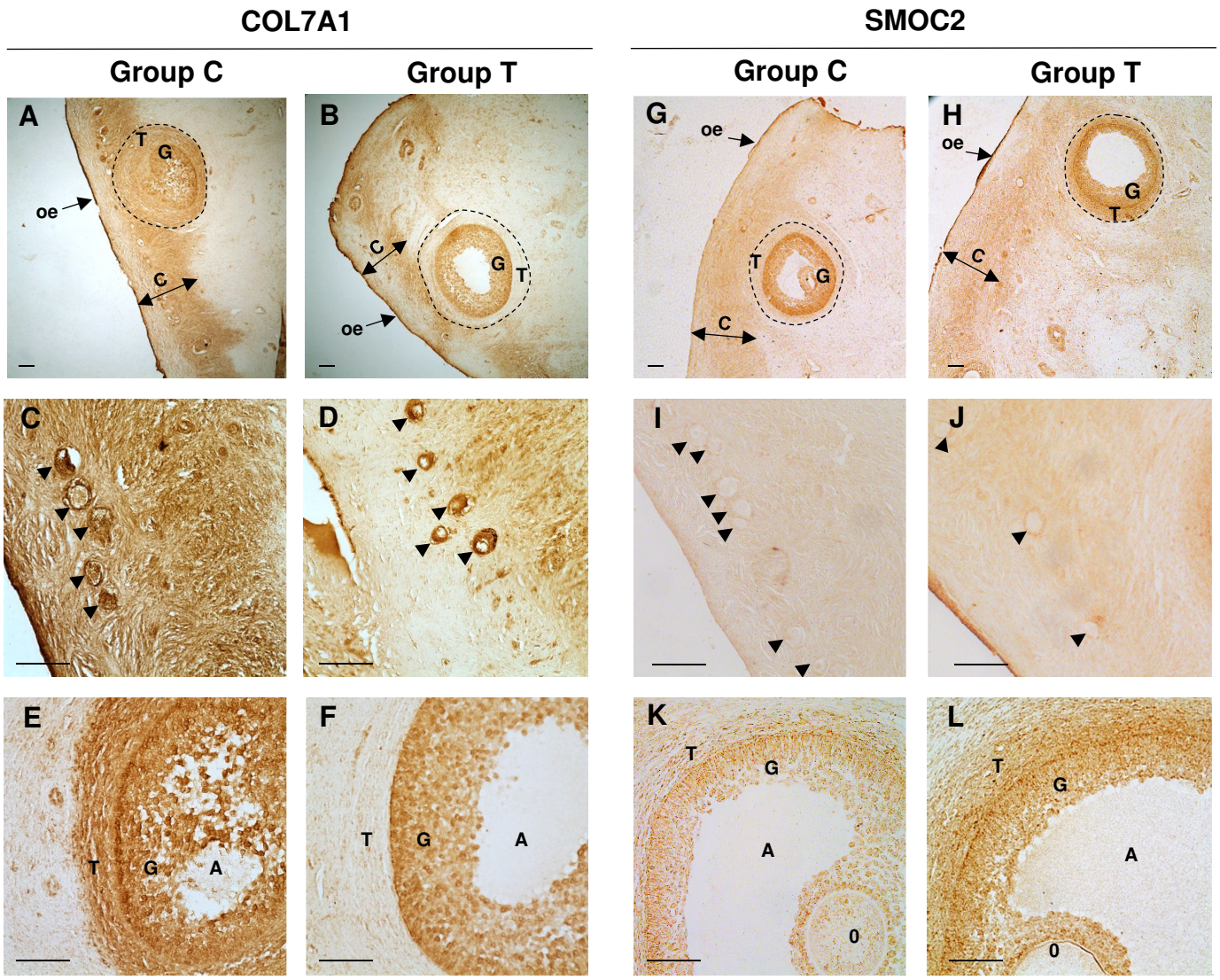
COL7A1
SMOC2
Group C
Group T
Group C
Group T
A
B
G
H
C
D
I
J
E
F
K
L
oe
T
G
C
A
0

Figure 7

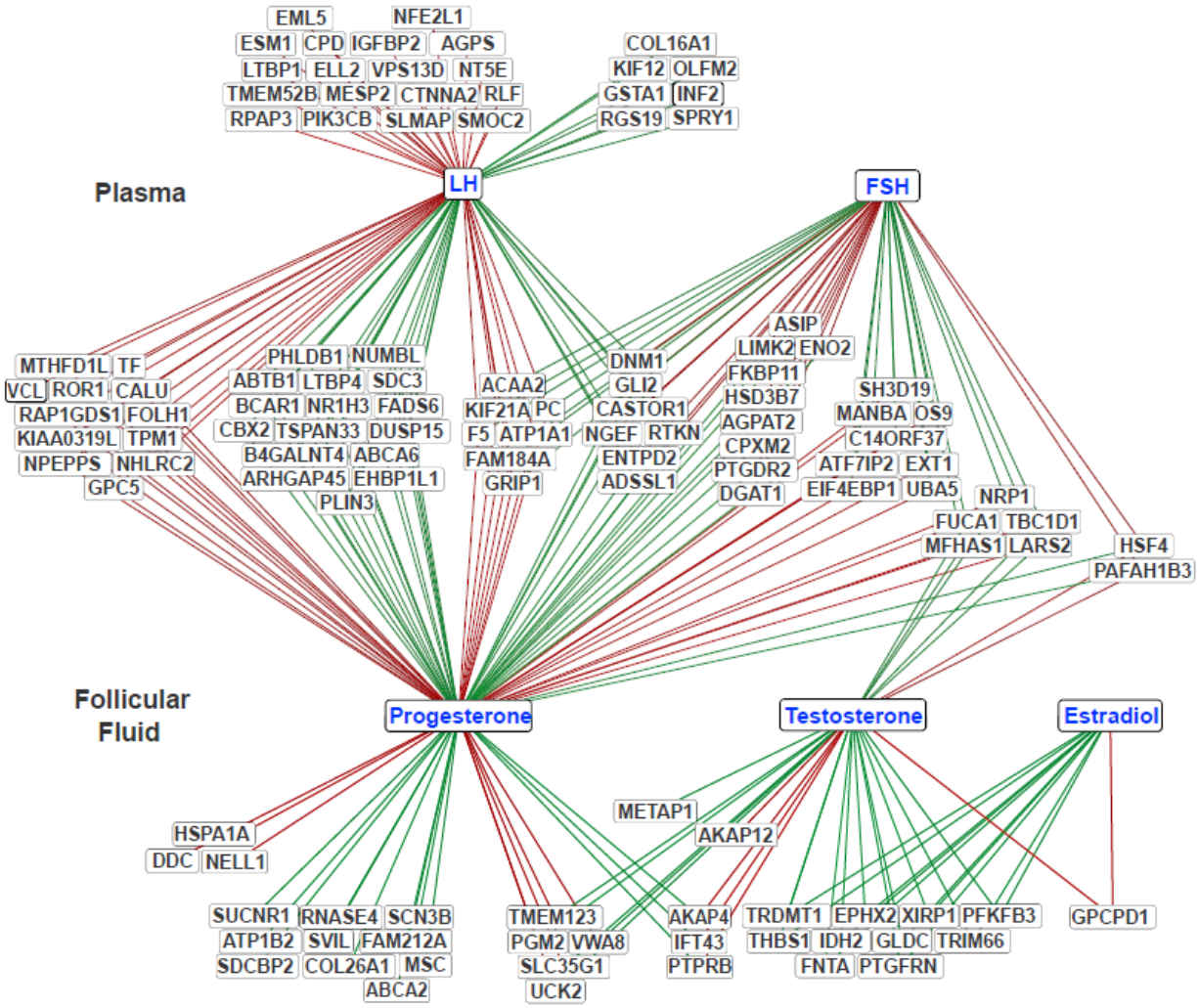
Plasma
Follicular Fluid
LH
FSH
Progesterone
Testosterone
Estradiol
EML5
NFE2L1
ESM1
CPD
IGFBP2
AGPS
LTBP1
ELL2
VPS13D
NT5E
TMEM52B
MESP2
CTNNA2
RLF
RPAP3
PIK3CB
SLMAP
SMOC2
COL16A1
KIF12
OLFM2
GSTA1
INF2
RGS19
SPRY1
MTHFD1L
TF
VCL
ROR1
CALU
RAP1GDS1
FOLH1
KIAA0319L
TPM1
NPEPPS
NHLRC2
GPC5
PHLDB1
NUMBL
ABTB1
LTBP4
SDC3
BCAR1
NR1H3
FADS6
CBX2
TSPAN33
DUSP15
B4GALNT4
ABCA6
ARHGAP45
EHBP1L1
PLIN3
ACAA2
KIF21A
PC
F5
ATP1A1
FAM184A
GRIP1
DNM1
GLI2
CASTOR1
NGEF
RTKN
ENTPD2
ADSSL1
ASIP
LIMK2
ENO2
FKBP11
HSD3B7
AGPAT2
CPXM2
PTGDR2
DGAT1
SH3D19
MANBA
OS9
C14ORF37
ATF7IP2
EXT1
EIF4EBP1
UBA5
NRP1
FUCA1
TBC1D1
MFHAS1
LARS2
HSF4
PAFAH1B3
HSPA1A
DDC
NELL1
SUCNR1
RNASE4
SCN3B
ATP1B2
SVIL
FAM212A
SDCBP2
COL26A1
MSC
ABCA2
TMEM123
PGM2
VWA8
SLC35G1
UCK2
METAP1
AKAP12
AKAP4
IFT43
PTPRB
TRDMT1
EPHX2
XIRP1
PFKFB3
THBS1
IDH2
GLDC
TRIM66
FNTA
PTGFRN
GPCPD1

Figure 8